# Hikurangi Margin Subduction Thrust, Post-Workshop Fieldtrip: Late Quaternary Upper Plate Deformation in the Southern Wairarapa Valley and Palliser Bay

May 15, 2010

Timothy Little[1]
Nicola Litchfield[2]

[1]Victoria University of Wellington
[2]GNS Science, Lower Hutt

**Frontispiece a:** Photograph taken from the top of the marine terrace above Ngawi (foreground), near Cape Palliser, looking north. The marine terraces (right hand side) are covered in alluvial fan deposits, but can be correlated all the way back into Palliser Bay, decreasing in altitude from ~200 m at Ngawi, to ~40 m at Lake Ferry. The mechanisms responsible for uplift of these terraces will be discussed. This photograph was taken near Stop 4 of this fieldtrip.

**Frontispiece b:** Photograph of the Wairarapa Fault, looking northward across the town of Featherston (photo by Lloyd Homer, GNS Science). Much of this scarp displaces the post-Last Glacial Maximum "Waiohine" terrace surface (green paddocks) in an up-to-the-NW sense. Stop 1 of this field trip is located just to the south of this image.


STOP 1
STOP 2
STOP 3
STOP 4
GNS
Hotel
WELLINGTON
LOWER HUTT
UPPER HUTT
PORIRUA
PETONE
WAINUIOMATA
Lake Wairarapa
Martinborough
Greytown
Palliser Bay
Cape Palliser
Turakirae Head
Baring Head
Sinclair Head
Pencarrow Head
Cape Terawhiti
Mana Island
10 5 0 10 km
41°10'S
41°20'S
41°30'S
174°40'E
174°50'E
175°0'E
175°10'E
175°20'E
175°30'E

**Trip Summary**

This fieldtrip highlights new observations and interpretations on the southern part of the Wairarapa Fault zone, a major dextral-oblique fault that probably merges with the Hikurangi subduction interface at depth; and along the southern coast of the North island, where last interglacial marine terraces have been differentially uplifted above (currently) the locked part of the subduction interface.

We first examine some 15 - 18.5 m dextral-slip displacements at several sites near Pigeon Bush that have been attributed to the 1855 earthquake; a very large displacement that may have been accompanied some rupturing of the subduction interface.

Second, on the south coast at Palliser Bay we will walk up Wharekauhau Stream (and time permiting, Te Mahonge Stream) paying special attention to near-coastal exposures of the Wharekauhau thrust, a conspicuous (albeit inactive) element in the Wharekauhau fault system. The Wharekauhau thrust is a major contractional fault that places Mesozoic "basement" rocks (Torlesse Terrane) on top of variably tilted, late Quaternary marine deposits and fluvial gravels. Recent work (structural geology and $^{14}C$ and Optically Stimulated Luminescence dating) suggests that the thrust underwent a period of very rapid motion (accruing >220 m of heave) during the period ~71-14 ka, corresponding to a horizontal shortening rate of >4 mm/y. This was >1/3 of the total Pacific-Australia margin-perpendicular plate motion rate. At that time, the fault moved in a direction subparallel to the Pacific-Australia plate motion rather than parallel to other adjacent upper-plate strike-slip faults, implying that the thrust was kinematically linked to slip on the subduction interface.

Stops 3 and 4 examine uplifted Pleistocene marine terraces preserved semi-continuously along the Palliser Bay Coast, which form part of Dee Ninis's ongoing PhD Thesis. Preliminary dating and surveying suggest that individual terraces can be traced from the Wairarapa Fault to the east coast (~30 km straight line distance), recording uplift and tilting to the northwest. We will discuss potential uplift mechanisms, including rupture of the Hikurangi subduction interface.

**Introduction**

The Pacific-Australia plate boundary in the North Island of New Zealand accommodates oblique subduction of oceanic crust along the Hikurangi margin of the North Island, and oblique continental collision in the South Island (Fig. 1). In the southernmost North Island, the contemporary oblique plate convergence of ~42 mm/yr can be broken down into ~30 mm/yr of margin-orthogonal motion and ~28 mm/yr of margin-parallel motion and (Beavan et al, 2002). The margin-orthogonal component is accommodated by thrust faulting and related folding in the onshore and offshore parts of the Hikurangi Margin's upper plate, including in an offshore accretionary wedge consisting of NE-striking reverse faults and folds, and by contractional slip on the subduction megathrust beneath these faults, which is thought to be strongly "coupled" in the southern part of the North Island (Barnes and Mercier de Lépinay, 1997; Barnes et al., 1998; Barnes and Audru, 1999; Nicol et al., 2002, 2007). The margin-parallel component of plate motion is accommodated by dextral-slip on the NNE-striking faults of the North Island Dextral fault belt (NIDFB), including the Wellington and Wairarapa faults (e.g., Beanland, 1995; Van Dissen and Berryman, 1996; Mouslopoulou et al., 2007), by clockwise vertical-axis rotation of eastern parts of the North Island (e.g., Wallace et al., 2004; Nicol et al., 2007; Rowen and Roberts, 2008), by strike-slip on active ENE-striking structures in Cook Strait (such as the Boo Boo Fault), and by oblique-slip on other, NE-striking offshore faults (Barnes and Audreu, 1999; Nicol et al., 2007). Seismicity data suggest that faults of the NIDFB, including the Wairarapa fault, intersect the subduction megathrust at depths of 20-30 km beneath the southernmost part of the North Island (e.g., Reyners, 1998). GPS geodetic data suggest that this segment of the subduction interface is currently "locked" and is accumulating elastic strain (Wallace et al., 2004).

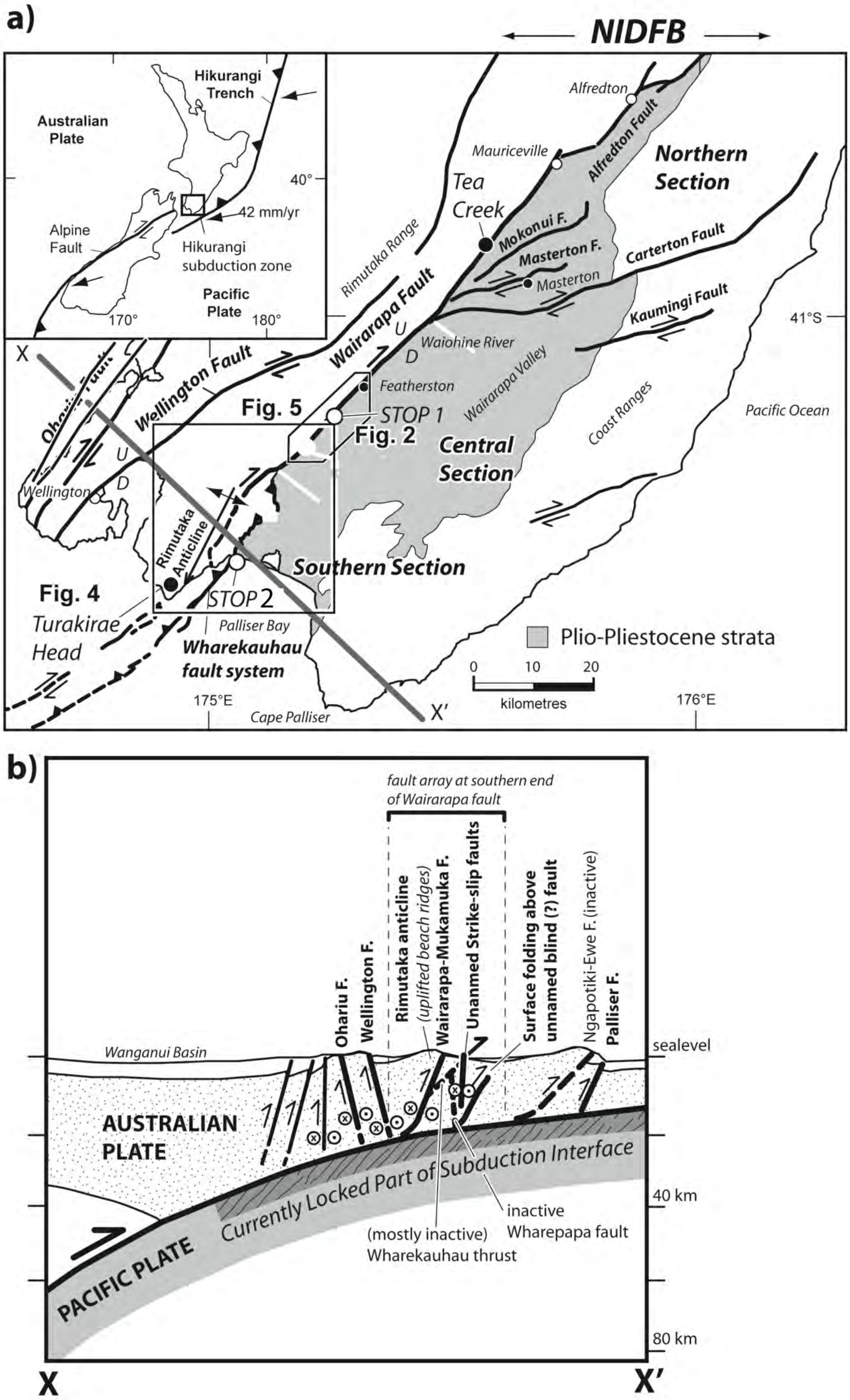


**Figure 1.** a) Tectonic index map showing major active faults and other structures of the southern North Island, New Zealand (largely after Begg & Johnston, 2000; Lee and Begg, 2002; and Barnes, 2005), and location of field trip stops sites along the Central and Southern sections of the Wairarapa fault. Inset on upper left shows contemporary plate tectonic setting of New Zealand (plate motions from Beavan, 2002). b) Schematic cross-section X-X' (position of currently locked part of subduction interface after Wallace et al., 2004).

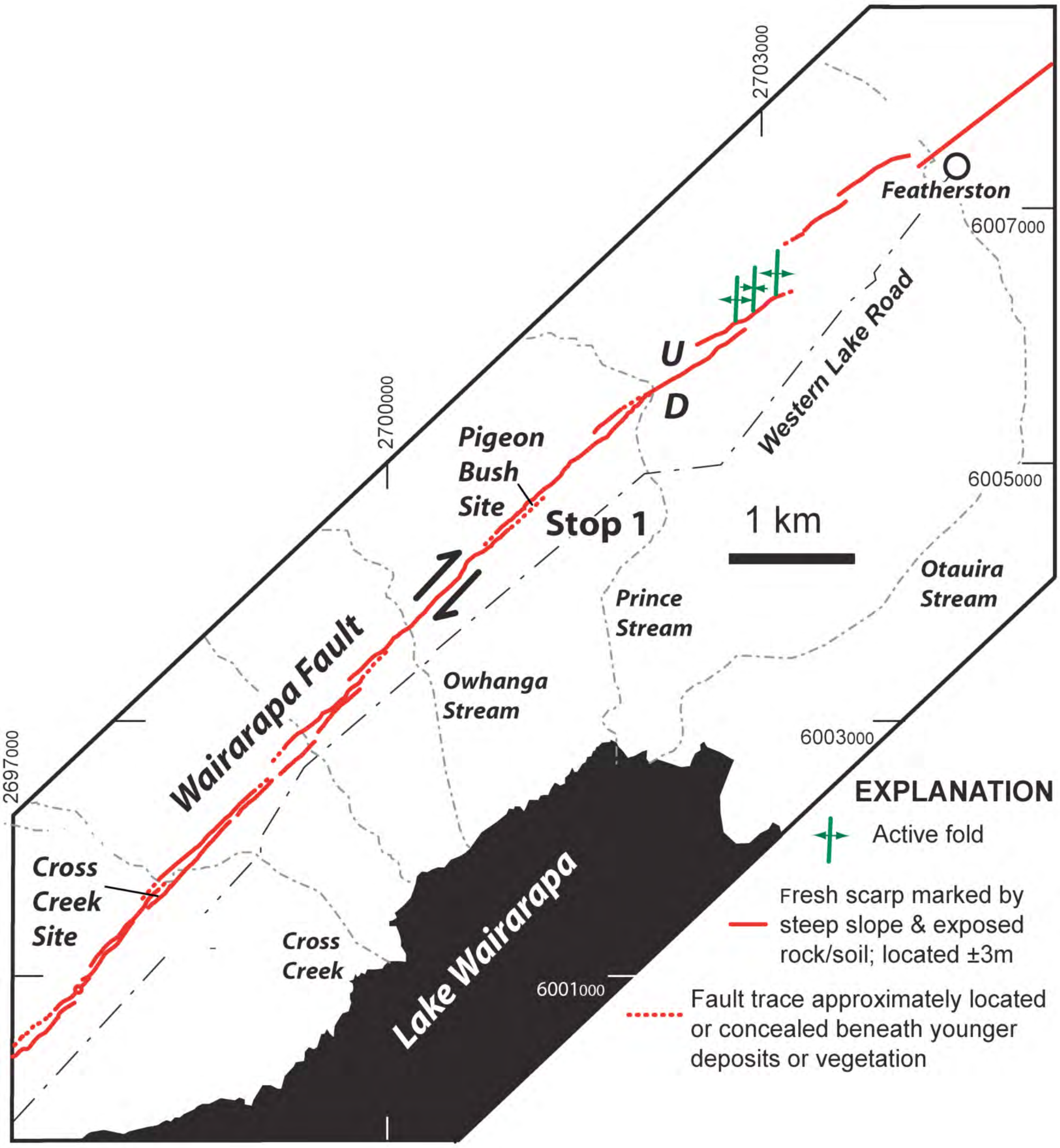


**Figure 2.** Fault traces along a southern part of the central Wairarapa Fault, south of Featherston (from Rodgers and Little, 2006), showing location of Stop 1 (Pigeon Bush area).

The Wairarapa fault is interpreted to have been initiated in the Pliocene as a reverse fault and reactivated as a strike slip fault at ~1-2 Ma in response to a clockwise vertical-axis rotation of the forearc relative to the Pacific Plate (Beanland, 1995; Beanland and Haines, 1998; Kelsey et al., 1995). The Wairarapa fault is the easternmost strike-slip fault in the NIDFB; whereas farther to the east, the structural style is dominated by margin-perpendicular shortening (folding and reverse faulting), a combination of which has uplifted the Aorangi Range on the SE coast of the North Island (Formento-Trigilio et al., 2002; Nicol et al., 2002). Dipping steeply to the northwest, the Wairarapa Fault bounds the eastern side of the Rimutaka Range, marked by a topographic step between the ranges and the subdued alluvial plain of the Wairarapa basin to the east. The central section of the fault is typically complex at the surface, including 250-500 m wide zone of mostly left-stepping *en echelon* traces and/or deformational bulges that have been active in the late Quaternary (Grapes and Wellman, 1988; Rodgers and Little, 2006) (Frontispiece a and Fig. 2). The northern section of the fault is marked by a series of dextral-slip splays (e.g., Carterton Fault) that bifurcate eastward away from the main trace of the Wairarapa fault farther to the west (Fig. 1). This main trace extends northward as far as Mauriceville South of Lake Wairarapa, the southern section of the fault includes a western strand that continues southwestward into the Rimutaka Range; and an eastern strand, that steps eastward ~5-6 km before deflecting back to a NNE-SSW strike and bordering the range front as far as the southern coast (Grapes and Wellman, 1988; Begg and Mazengarb, 1996; Begg and Johnston, 2000) (Fig. 1).

We refer to the faults that comprise eastern strand of the greater (southernmost) Wairarapa fault zone as being the "Wharekauhau fault system". This strand has previously been interpreted to consist chiefly of an active thrust fault termed "the Wharekauhau thrust" that is also inferred to have been a locus of strike-slip surface rupturing during the 1855 earthquake. For this field trip we will restrict the term "Wharekauhau thrust" to a specific low-angle thrust fault. Well exposed near the Palliser Bay coast, this thrust emplaces Torlesse terrane rocks in its hangingwall over Quaternary sediments in its footwall. We infer this major fault to be inactive and not to have ruptured (at least as a thrust) in 1855, although some northern parts of the Wharekauhau fault system were locally reactivated during the Holocene,

The top surface of a post LGM abandoned fan complex (the "Waiohine surface") has been widely mapped along the western side of the Wairarapa Valley, where it dips gently eastward beneath the surface of Lake Wairarapa (Begg and Johnston, 2000; Lee and Begg, 2002). On the western margin of the lake, the age of this surface has recently been bracketed by $^{14}C$ dating of samples collected on both sides of its gravel tread at a single site (Cross Creek trenching site, south of Pigeon Bush). These results constrain fan abandonment to have taken place soon after 12.4 ka. Based on the stratigraphic context of the samples collected in gravel close below the terrace tread, these authors infer an abandonment age of 12-10 ka for the surface at that locality. This age, together with reported lateral offsets of 99-130 m relative to that terrace surface (in particular at Waiohine River, Fig. 1), suggests a Late Quaternary dextral-slip rate for the Wairarapa Fault of 8-15 mm/yr (Wang and Grapes, 2007; Little et al., 2009). A slip rate has never been measured for the Wharekauhau thrust, or for any other faults in the Wharekauhau fault system.

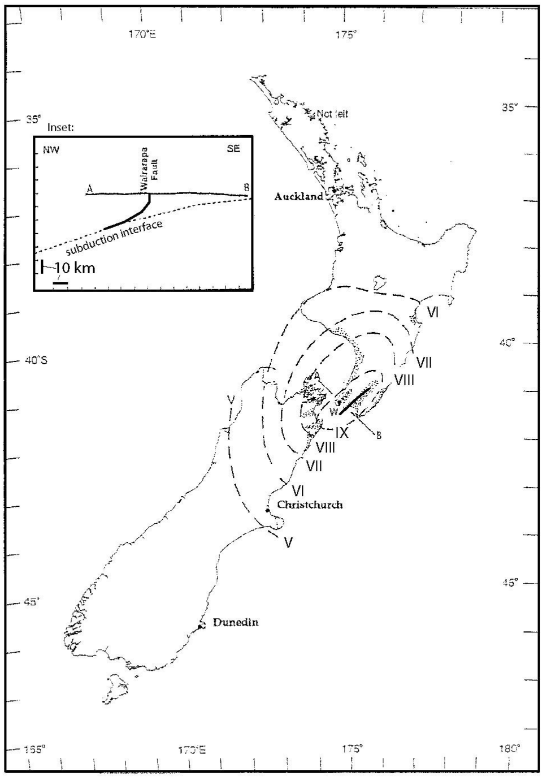


**Figure 3.** Isoseismal map of 1855 earthquake (from Grapes and Downes, 1997) showing area of ground damage (stippled) and rupture along Wairarapa Fault. W = Wellington. Inset- cross-section along A-B showing inferred shape and extent of Wairarapa Fault rupture at depth during 1855 (after Darby and Beanland, 1992).

**Figure 4.** Oblique aerial view, looking northeast, of the uplifted beach ridges at Turakirae Head. The ridges have been dated using $^{14}C$ (radiocarbon) and $Be^{10}$ surface exposure dating techniques (Hull and McSaveney et al. 2006). Here, 2 km SW of the axis of greatest uplift in 1855, BR2 was raised 4.7 m in 1855, BR3 was raised 7.1 m in the event prior to 1855, BR4 was raised 3.7 m in the earthquake before that, and BR5 was raised 3.4 m in the earliest Holocene earthquake recorded here. In the distance, at least two raised marine benches (analogous with the Holocene bench in the foreground) can be seen in the coastal profile. Suggested age correlations for these benches (Ota et al., 1981) were based on high sea level stands of the international sea level curve.

## The 1855 Earthquake

The Wairarapa Fault east of Wellington, New Zealand ruptured on January 23, 1855, resulting in ground shaking, landsliding (especially in the Rimutaka Range), regional uplift, tsunamis, and >120 km of ground rupturing (Grapes, 1999; Grapes and Downes, 1997). Historic accounts indicate that the 1855 earthquake ruptured the Wairarapa Fault, Fresh scarps attributed by Grapes (1999) to the 1855 rupture are preserved in the landscape from near the coast to Mauriceville, as much as ~88 km northward (Fig. 1). More recent work suggests that slip in 1855 may also have ruptured a northward continuation of the Wairarapa Fault, the Alfredton Fault: scarps along that fault were rejuvenated sometime after 250 - 330 years BP, implying that the 1855 rupture may have extended to Alfredton, as much as 30 km beyond Mauriceville (Schermer et al., 2004). These data suggest that the onshore part of the 1855 rupture could have been as long as ~120 km. Modern estimates of magnitude based on dislocation modeling of the observed distribution of vertical uplift, and on the felt extent of ground shaking (Fig. 3) suggest a moment magnitude ($M_w$) of 7.9 to 8.2 (Darby and Beanland, 1992; Dowrick, 1992), whereas revised measurements of surface offset and inferred rupture size suggest an $M_w$ of at least 8.2 to 8.3 (Little and Rodgers, 2005; Rodgers and Little, 2006). This makes the 1855 earthquake by far the largest seismic event in modern New Zealand history (Van Dissen and Berryman, 1996). One goal of this field trip (Stop 1) is to provide participants with a chance see the fault rupture and slip that took place during a recent (in this case, ~150 year old) earthquake. At Stop 1 we will examine a place (Pigeon Bush and environs) where "smallest" strike-slip offsets as high as 15 -18.5 m have been measured and attributed to that historic earthquake (Rodgers and Little, 2006).

The interaction of the subducting plate interface and faults of the NIDFB is poorly understood, although GPS modelling suggests that the megathrust is currently locked and is also loading crustal faults at depth beneath the southern North Island (Darby and Beavan, 2001; Wallace et al., 2004). Rodgers and Little (2006) argued on the basis of the remarkably high co-seismic slip during the 1855 rupture, and especially its unusually large displacement/length ratio, that this earthquake co-ruptured a part of the subduction interface with which it was contiguous down-dip, an inference that is consistent with elastic dislocation modeling of the vertical component of motion during that earthquake, albeit not required by it (Beavan and Darby, 2005). The only way such modeling was able reproduce the large amplitude of uplift at Turakirae Head in combination with the short wavelength of that uplift signal was by imposing a reverse-slip motion on a fault nearby to Turakirae Head (e.g., on the Muka Muka Fault, Fig. 11). This large co-seismic uplift (up to a maximum of 6.4 m at the crest of the Rimutaka anticline, Fig. 1) has been inferred from the height of a beach ridge near Turakirae Head (labeled "BR 2" in Fig. 4). Dating of this beach ridge and the three other beach ridges, above it, led McSaveney et al. (2006) to infer the timing the last four earthquakes on the Wairarapa fault, and to infer a mean recurrence interval of ~2200 yrs for Wairarapa Fault earthquakes. More recently, Little et al. (2009) have undertaken paleoseismic trenching studies to determine the chronology of paleoearthquakes on this fault, and to compare this record of fault rupturing with the geomorphic record of coastal uplifts near Turakirae Head.

**Surface Expression of Central Segment of the Wairarapa Fault Zone, South of Featherston**

Heading South from Featherston on Western Lake Road, you note the scarp of the Wairarapa fault off your right. Typically it is located near the upper edge of the grazed paddock land, and below the heavily bushed foothills of the Rimutaka Range (Frontispiece b)

Although within a few decades of 1855 the land was largely deforested and converted to grazing land, and despite the passage of 150 years, many of the scarps in the Featherson-Lake Wairarapa region are still remarkably fresh-looking, and are likely to be of 1855 age. These scarps locally retain slopes of 30-70° – steep enough to expose planar outcrops of the terrace alluvium. Other probable 1855 scarps lack such steep faces, but demonstrably cut and displace small landforms, such as shallow rills. Scarps higher than ~20 m occur on the limbs of the anticlinal bulges. These are typically mantled by landslides. Where the fault is expressed by multiple overlapping segments at the surface, each not necessarily experiencing slip at the same time, recognition of the 1855 increment of slip becomes difficult or impossible.

In the southern Wairarapa Valley, the fault zone strikes ~046° overall but is slightly arcuate in detail (Figs. 2 & 5), and one can define three relatively straight sections that are bounded by Owhanga Stream and Cross Creek. The most prominent scarps of the Wairarapa Fault border the eastern edge of its zone, where they cut Torlesse Terrane bedrock and late Quaternary alluvium, especially the "Waiohine" surface, which is typically displaced vertically by 5-20 m across the fault zone. Because the "Waiohine" surface is an old surface, these scarps represent many Wairarapa Fault ruptures. Most of these scarps are linear, ~1-3 km long, and discontinuous (Fig. 2). The fifteen individual strands that Rodgers & Little (2006) mapped in the area south of Featherston are 1200±700 m long and define a distinct, left-stepping, *en echelon* pattern. The overlapping parts of the stepovers are typically 400-600 m long and 20-200 m wide. Some of these compressional stopovers coincide with uplifted fault blocks, whereas others bound an active anticline or tectonic bulges, expressed in the landscape by the warping of the alluvial terraces, and by laterally varying scarp heights. Right-stepping *en echelon* zones are rare but result in small closed depressions and bogs less than a few tens of metres in width. Both situations cause along-strike variations in slip and locally complicate the interpretation of 1855 displacement.

Along the western side of the Wairarapa Fault zone, at higher elevation and closer to the topographic front of the Rimutaka Range, other laterally continuous, and perhaps now inactive fault strands with more subdued or diffuse scarps can be traced using air photographs. This observation suggests faulting may have stepped eastward away from the range front with time.

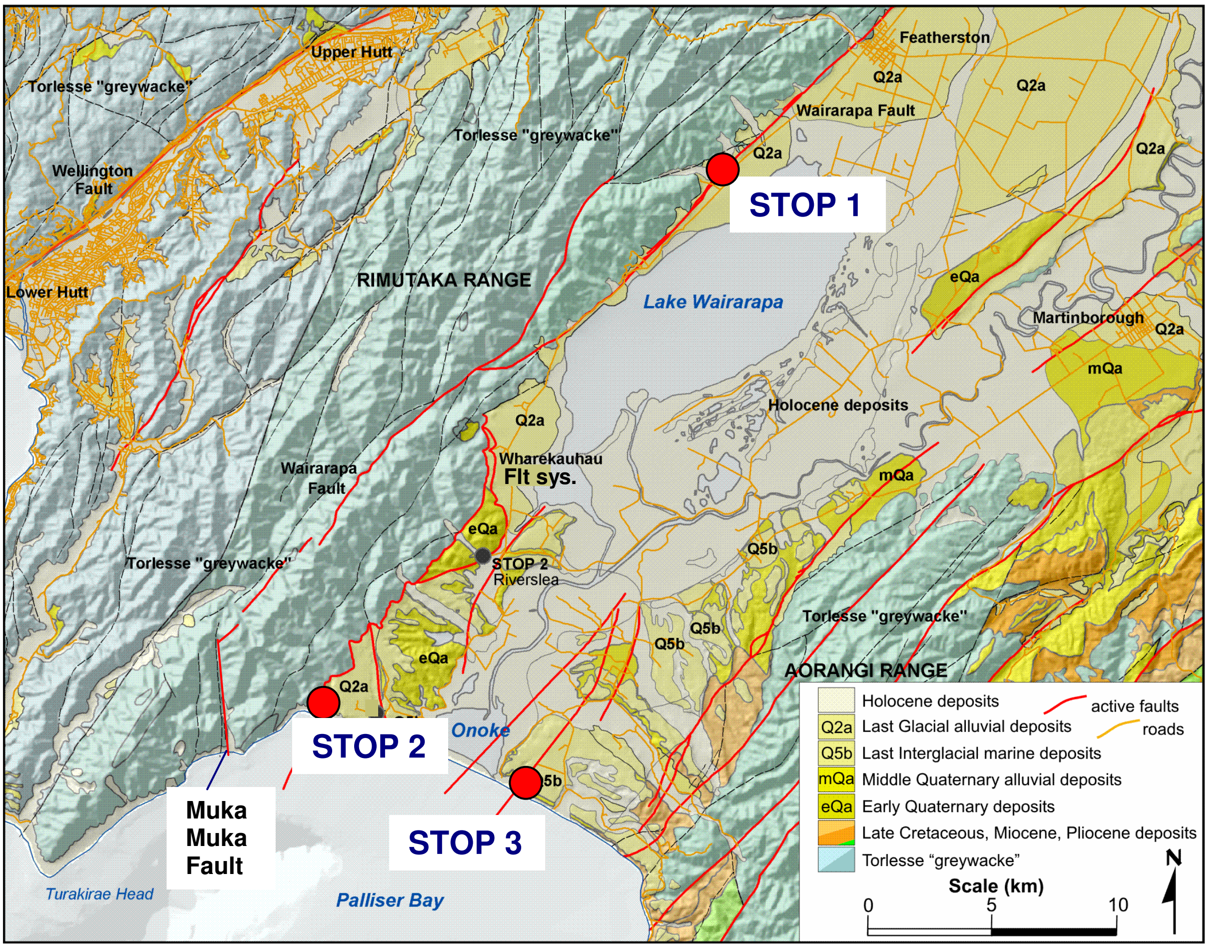


**Figure 5.** Geological map of the southern Wairarapa (from Begg & Johnston, 2000). The locations of Stops 1, 2 and 3 are shown. Note location of Turakirae Head (shown in photo of Fig. 4). Some of the splaying of the Wairarapa Fault and the Wharekauhau fault systems can be seen. The Wharekauhau Thrust is exposed near the coast at Stop 4, where it dips gently (20-30°) to the west, suggesting that the two faults merge at depth.

## STOP 1. 1855 Rupture Trace in the Pigeon Bush Area (Pigeon Bush Localities 1, 2, and 3)

*Park the vehicles at Pigeon Bush 1 and walk to Pigeon Bush localities 2 and 3. We will return on foot to the vehicles after approximately 1 hour.*

### *Pigeon Bush Locality 1*

Pigeon Bush 1 is justifiably the most famous geological site on the Wairarapa Fault. There, Grapes and Wellman (1988) interpreted two well-preserved, beheaded streams as evidence of dextral offset of a small stream gully cross-cutting the Wairarapa Fault during two sequential earthquake events, most recently in 1855. The fault is marked by a SE-facing scarp cut into Waiohine gravel that is ~6 m high. On the northern side of this scarp, the uplifted “Waiohine” terrace is tilted SW, whereas on its southern side it is partly buried beneath a ~1 m-thick layer of silt (and by younger swamp deposits). The silt was incised by the two channels. Wang and Grapes (2007) dated two samples of the silt by OSL methods, obtaining ages of 7.0±0.5 ka and 4.3±0.5 ka.


**Figure 6.** Google Earth Image of Pigeon Bush Localities.

On the uplifted (NW) side of the fault, the "Waiohine" gravels have been back-tilted to the southwest by ~5° on the limb of an anticlinal bulge that crests to the NE of this site. Over time, this tilting has diverted some of the stream's headwaters southward into an adjacent stream. Thus the gorge on the up-thrown side of the scarp now seems disproportionately deep with respect to the small, low-discharge stream that currently flows within it. This is important because the stream flows through an entrenched gorge that is, in a sense, partially abandoned and thus little modified since its displacement along the fault.

As recognized by Grapes and Wellman (1988), the well-preserved geomorphology of the beheaded streams supports the idea that this younger increment of slip accrued during a single event, rather than as a composite displacement involving one or more intermediate stages. Both beheaded channels on the downstream side of the fault retain a linear morphology all the way up to the fault, where they are orthogonally truncated against the scarp. Similarly, the source gorge on the upstream side does not widen significantly at the fault, but remains narrow, linear, and fault-transverse all the way to

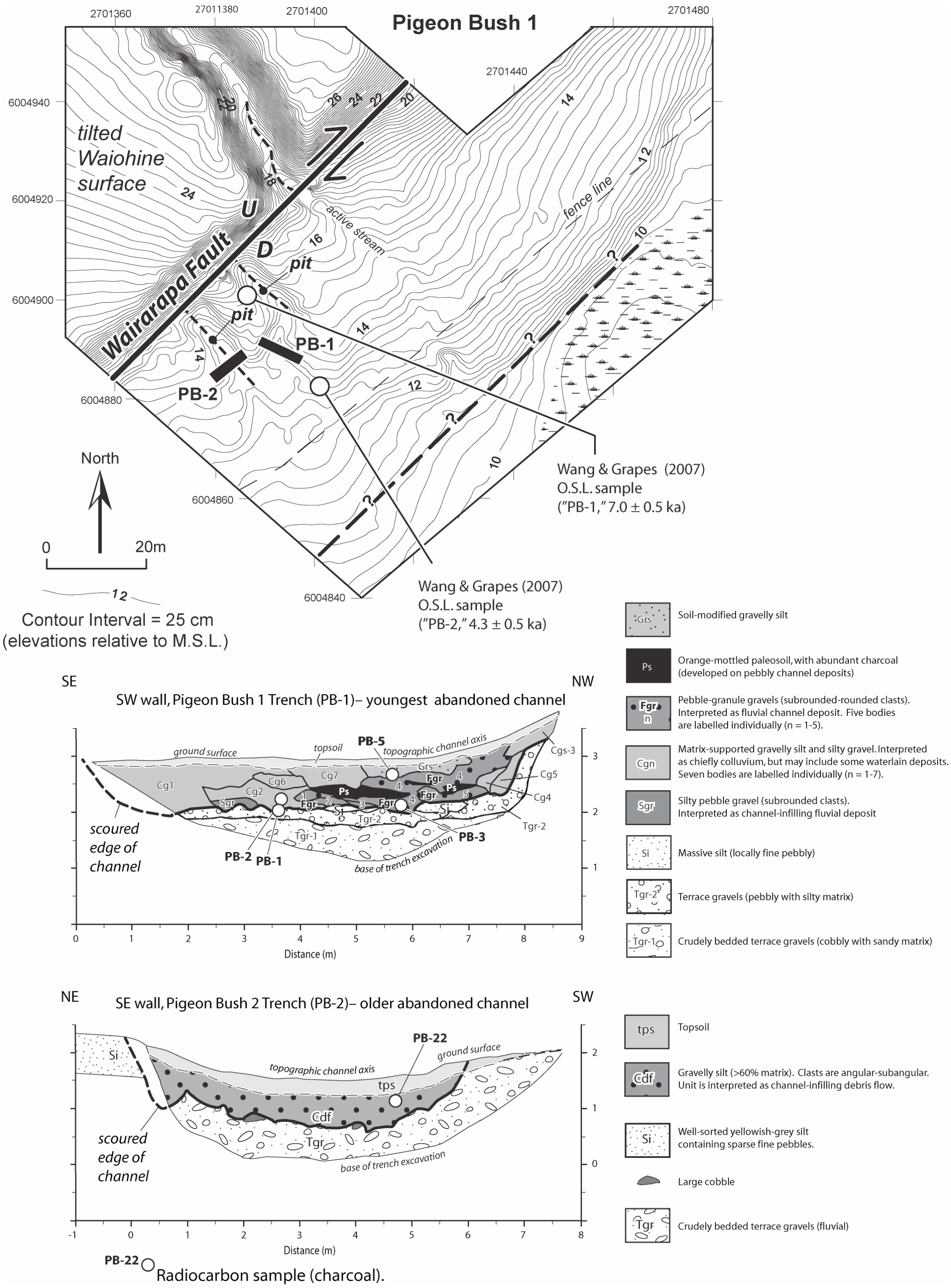


**Figure 7.** Microtopographic map of the Pigeon Bush 1 site, showing beheaded channels displaced by slip on the Wairarapa Fault. Map is based on a survey data set consisting of >10,000 points (Rodgers & Little, 2006). Trench Logs are from Little et al. (2009). All $^{14}$C ages (including two from the pits dug by Rodgers and Little, 2006) yielded similar ages, suggesting a bush fire that took place at, or soon after, ~546-497 cal yr. BP (1404-1453 cal. yrs, AD), perhaps in response to Maori burning.

the scarp. There is no evidence for a paleo-channel having run along the fault scarp between the modern stream and either of the abandoned channels, as might reflect an intermediate phase of stream dog-legging induced by shutter ridge damming. According to Rodgers and Little 2006, the proximal beheaded channel has been displaced 18.7±1.0 m dextrally and ≥1.25±0.5 m vertically relative to the deeply entrenched active channel on the upstream side of the fault. The other channel is displaced 32.7±1.0 m dextrally and ≥2.25±0.5 m vertically from its source. This larger offset suggests that the older, distal channel had previously been displaced by 14.0±1.0 m of dextral-slip and ~1.0 m vertical-slip prior to incision of the proximal abandoned channel. The vertical-slip estimates do not account for any post-slip incision of the upstream channel and so are minima. The ~18.5 m dextral-slip of the proximal channel is the largest coseismic displacement documented for any strike-slip earthquake globally. The next-largest is 14.6 m of strike-slip during the 1931 earthquake on the Keketuohai-Ertai fault in Mongolia (Baljinnyam et al., 1993).

Each of the last two earthquakes on the Wairarapa fault at this site resulted in abandonment of a stream channel immediately downstream of the narrow headwater gully and incision of a new channel in downstream continuity with that gully. Hoping to date the last two earthquakes, Little et al. (in press) excavated trenches PB-1 and PB-2 (Fig. 7) at right angles to each of the two channels to date their incision and abandonment. Trench PB-2 was cut orthogonally across the older of the two beheaded channels. Fluvial terrace gravels at the base are scoured beneath a ~1 m deep, channel-bounding unconformity. The channel is infilled by a massive, matrix-supported pebbly clay interpreted as a debris-flow. No fluvial deposits are present. A single piece of charcoal near the top of the debris flow (PB-22) yielded a $^{14}C$ age of 543-495 cal. yrs BP, which suggests that it is another element of the above-described burn population that had become entrained into the debris flow. The only fluvially deposited organic material that we found in either channel (charcoal) occurs as detrital particles within the fluvial deposits that infill the incisional scour beneath the youngest of the two beheaded channels. This channel was cut immediately after the penultimate earthquake. Thus our preferred age of charcoal-producing “burn event” (~546-497 cal yr. BP) provides a minimum age constraint for the penultimate earthquake at this site (event $Pb_2$). Historical data indicates that the youngest earthquake here (event $Pb_1$) took place in 1855.

***Pigeon Bush Locality 2***

This region is located <1 km northeast of Pigeon Bush 1 (Fig. 6). Here the fault is characterized by a scarp that coincides with an abrupt southeast-facing topographic step and two elongate topographic depressions. A second strand marked by a small, southeast-facing topographic step may occur to the southeast of the main one, and a third may be present ~100 m to the northwest, but neither of these coincides with any fresh scarps or has revealed any evidence of recent slip.

Two small streams are incised 1.0 to 4.5 m into the older terrace alluvium and are dextrally displaced across the fault (Fig. 8). Where the streams cross the fault trace they deflect abruptly to the southwest to flow parallel to the fault before deflecting back to the southeast again on the downthrown side of the fault. Linear axes were defined along

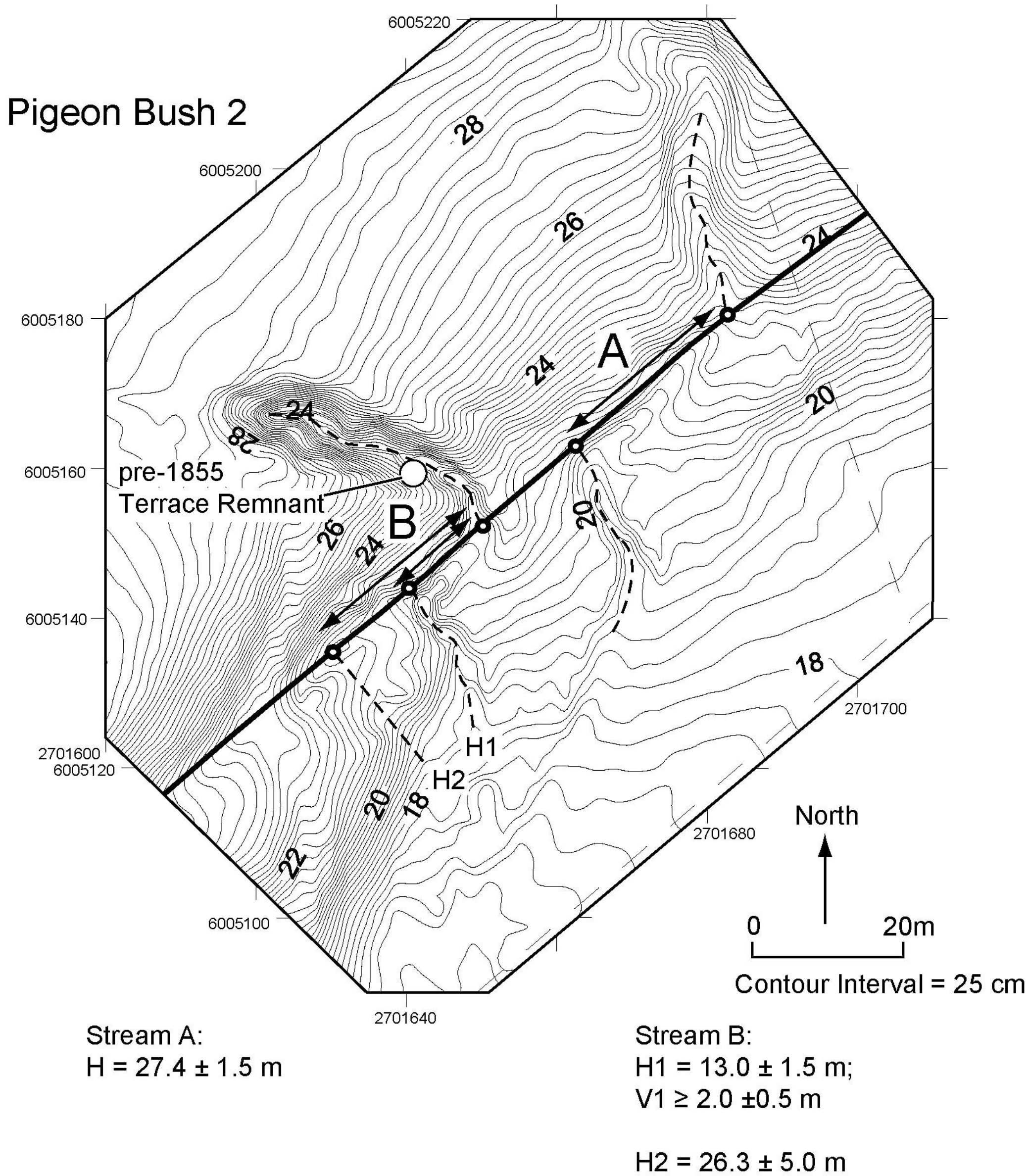


**Figure. 8.** Microtopographic map of the Pigeon Bush 2 site, showing channels displaced by slip on the Wairarapa Fault (from Rodgers and Little, 2006). See Fig. 6 for location.

these incised channels and their dextral offset was restored with the aid of a microtopographic map. A narrow fluvial terrace remnant is preserved on the NW side of the western of the two streams (Stream B). Its 0.75±0.25 m of incision by the modern stream on the NW side of the fault, and the 1.25±0.25 m of vertical-offset of stream channel B across the fault together suggest ~2 m of vertical-slip (interpreted as a minimum, as this sum does not account for any post-1855 deposition that may have partially infilled the channel on the on SE side). Dog-legging of this southwestern stream implies 13.0±1.5 m of dextral-slip, whereas dog-legging of the other active stream to the NE records 27.4 ±1.5 of dextral-slip. Following Grapes and Wellman (1988), we interpret the smaller stream offset to have accumulated in 1855 and the larger one to record a summation of slip during both 1855 and the next-older (penultimate) earthquake. This two-increment model of slip accumulation is strongly supported by recent discovery of a subtle abandoned stream channel on the downthrown side of the fault to the southwest of the SW active stream. The beheaded stream channel is dextrally offset by 26.3 ±5.0 m from its incised source: thus both of the small streams preserve evidence for a ~26-27 m horizontal slip, and one of the streams, similar to the nearby Pigeon Bush 1 site, also preserves evidence for a younger and smaller increment of offset.

***Pigeon Bush Locality 3***

Located about 300 m southwest of Pigeon Bush 1 (see Fig. 6) this is the site that Rodgers and Little (2006) described featuring a beheaded channel on the southeast side of the fault that has been dextrally offset relative to an active channel segment on the upstream side. At this locality (Pigeon Bush 3), the Wairarapa Fault zone is ~50 m wide, comprising a 2 m high, southeast-facing fault scarp to the southeast and a 2 m high, northwest-facing fault scarp to the northwest (Fig. 9). The southeast strand is characterised by a linear, southeast-facing topographic step, though it is unclear whether this segment slipped in 1855. The northwestern strand is continuous with the main scarp at Pigeon Bush 1, is similarly fresh-looking, and crosses a small stream, and displaces a small river terrace. This stream is now partly dammed by a dextrally displaced shutter ridge.

The small stream that flows across the northwestern fault strand has been diverted northeastward around the shutter ridge. Southwest of this fault strand, a 0.75 to 2.0 m deep wind gap (abandoned channel) is incised into the shutter ridge at an elevation ~2 m higher than the current level of the stream. Restoration of the western edge of this inactive, beheaded channel segment on the southeast side of the fault with the (also inactive) terrace riser on the northwest side of the fault indicates a dextral-slip of 15.1 ±1.0 m and vertical-slip of -1.8 ±0.5 m (up to southeast) across this strand. Recent incision of the terrace remnant on the upstream part of the fault suggests that despite its downthrown sense of local relative motion, this northwest fault block was uplifted relative to sea level in 1855, similar to other sites on that side of the Wairarapa Fault.

Between the offset (abandoned) channel and the active stream, the uphill-facing free face formed by the 1855 rupture plane is still remarkably well preserved. This near-vertical plane is only locally obscured beneath small fans of colluvial debris derived by the gravitational collapse of that free face during the past ~150 years.

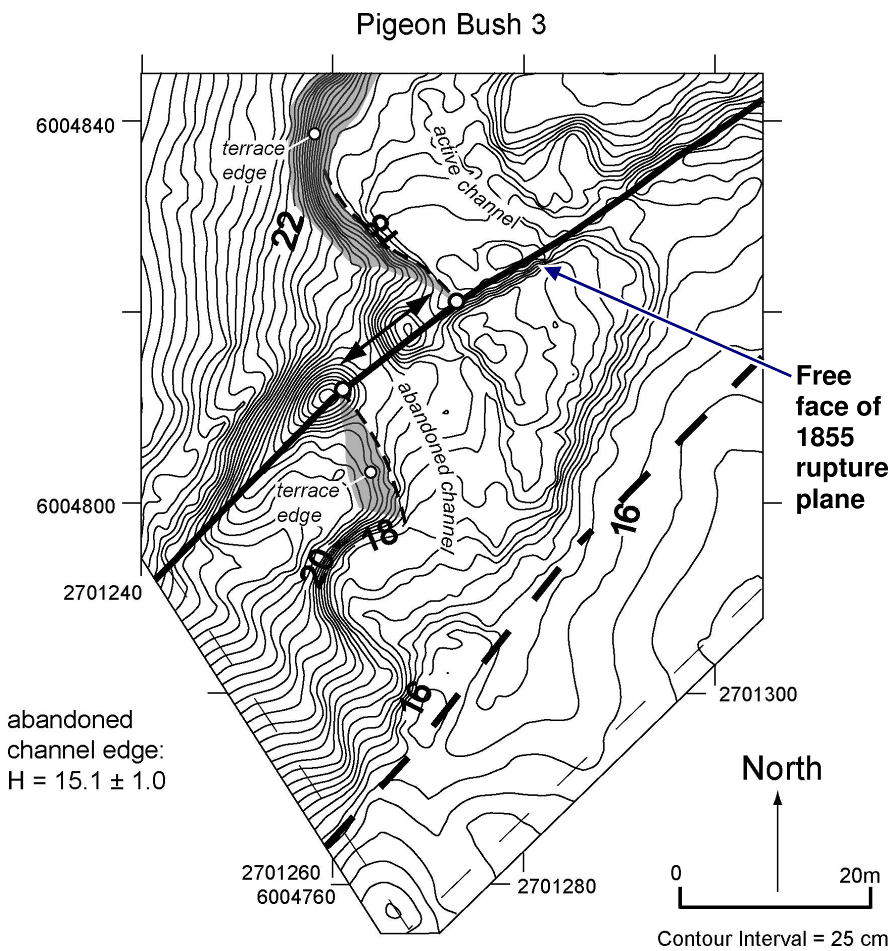


**Figure 9.** Microtopographic map of the Pigeon Bush 3 site, showing channels displaced by slip on the Wairarapa Fault. See Fig. 6 for location. From Rodgers and Little (2006).

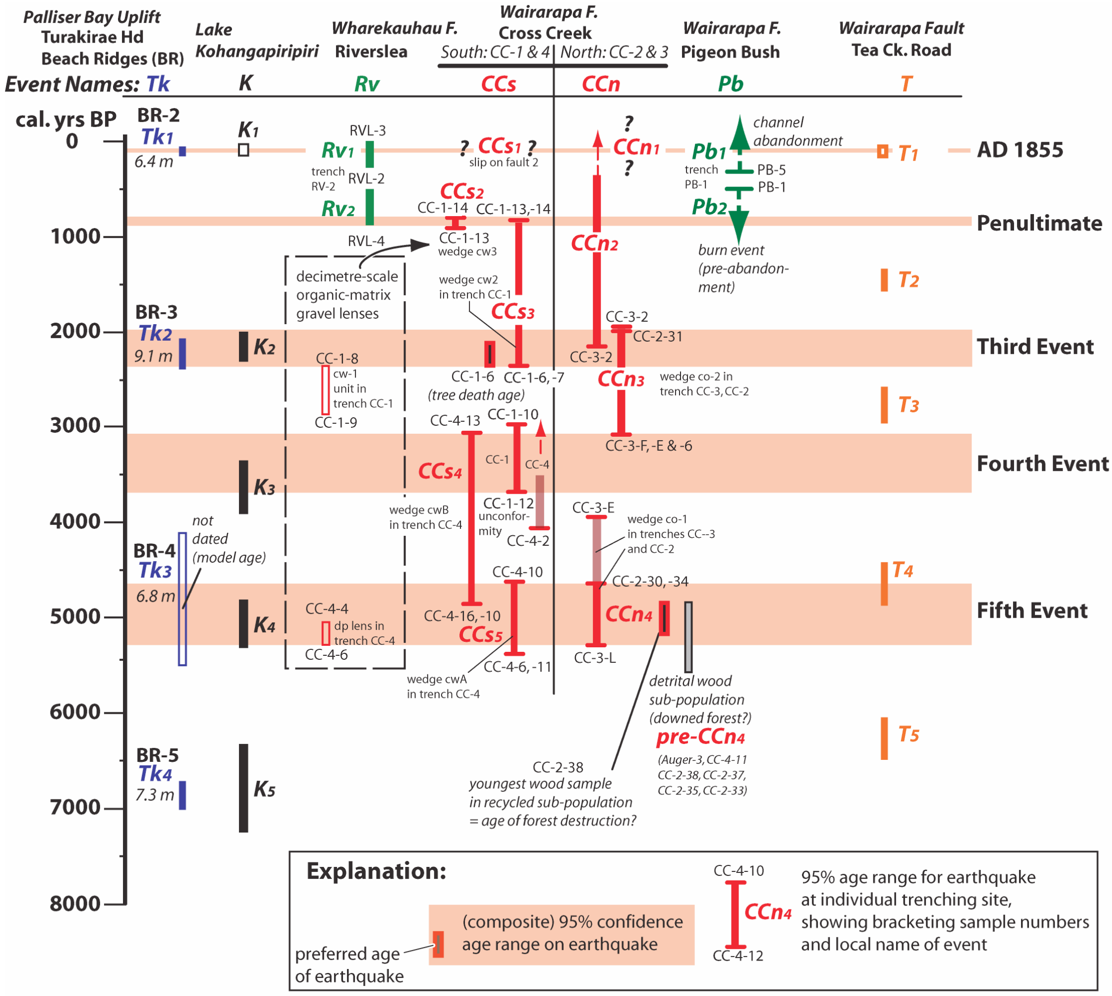


**Figure 10.** Time-space plot of surface-rupturing Wairarapa fault earthquake events inferred from all available types of paleoseismological data (from Little et al., 2009). Data for Tea Creek trench (events labelled, *T*) are from Van Dissen and Berryman (1996, and unpub. $^{14}$C data). Diatom-based paleoenvironmental data for coastal uplift events at Lake Kohangapiripiri (events, *K*, shown as solid black bars) are from Cochran et al. (2007). Uplift events near Turakirae Head on Palliser Bay (events, Tk, shown as open to closed blue bars) inferred from raised beach ridges (BR-1 to BR-5) are taken from McSaveney et al. (2006). Small numbers quoted in meters denote inferred single-event uplift magnitudes for a given event. For Palliser Bay data, these refer to the maximum uplifts near Turakirae Head as inferred by McSaveney et al. (2006). Name of key $^{14}$C samples that bracket the timing of rupture events in trenches (this study) are identified at maximum and minimum limits of error bars (95% confidence). Colored horizontal bands depict the maximum and minimum age range (at 95% confidence) for each earthquake event as derived from an analysis of the composite set of trench data and $^{14}$C results.

## *Late Holocene Rupturing History of the Southern Wairarapa Fault and Comparison to the Turakirae Head Beach Ridges*

By integrating the key stratigraphic and structural events observed in the eight paleoseismic trenches (2 at Pigeon Bush, 4 at Cross-Creek and 2 at Riverslea, see Figs. 2 and 5) and by dating and correlating these using the 40 new $^{14}$C samples, Little et al.

(2009) interpreted a composite surface rupturing history that included at least five earthquakes on the southern part of the Wairarapa fault since ~5.2 ka (Fig. 10). McSaveney et al. (2006) identified and dated the uplift and stranding of four late Holocene beach ridges at Turakirae Head. Three of these are younger than ~5.2 ka. Each of these corresponds to one of our independently determined Wairarapa fault rupturing events (Fig. 10). Two of our trench-determined fault rupturing events cannot be matched to a corresponding beach ridge at Turakirae Head. These are the Penultimate Event and Fourth Event. Our comparison between the trench-based earthquake rupturing history of the Wairarapa Fault and the sequence of raised beaches at Turakirae Head leads us to conclude that flights of uplifted gravel beach ridges may provide an incomplete record of paleoearthquakes on adjacent reverse-oblique faults. The paper by Little et al. (2009) suggests several processes, both tectonic and non-tectonic, that might result in the geomorphic "omission" of one or more beach ridge from an uplifted sequence. These include: a) variable rupture geometries at the southern end of the Wairarapa-Wharekauhau fault systems (a zone of particularly complex fault splaying and folding in the near-surface, Fig. 1b), with some earthquakes causing only a small uplift at Turakirae Head and no discrete beach ridge being raised; and b) landward retreat of an active storm berm (perhaps during a particularly stormy interseismic periods) to cause its overwhelming of, or amalgamation with, the next highest beach ridge (thus causing an apparent omission of a beach ridge).

## Optional Stop at location of 127 ± 10 ka OSL sample of last-interglacial marine sand on road-cut (For location see Fig. 11)

On our drive along Western Lake Rd, note how it skirts the edge of the hills and the flat swampy country to the west of Lake Onoke. There is evidence that the road traverses around sandy berms that bounded a former Holocene estuary, the last remnant of which is Lake Onoke itself. Lake Pounui, a small lake nestling within these hills is ponded behind an active fault, the Battery Hill Fault. This can best be seen where it displaces a prominent terrace surface by about 10 m, its eastern side upthrown, and it probably dips to the east as a reverse fault. Note that on your left (east side of the fault) the road exposes uplifted gravel and silt alluvial deposits of the early to middle Quaternary Ahiaruhe Formation.

A several-meter thick Last Interglacial marine deposit (well-sorted and rounded sands and pebble gravels) rests unconformably above the fluvial Ahiaruhe Formation. These beach(?) deposits, in turn, are overlain a considerable thickness (~10+ m) of younger fluvial gravels that continue to the top of the terrace tread. This composite (marine + fluvial) terrace, called unit "Q5a" by Begg and Johnston (2000), can be tracked to the east to beyond Lake Ferry (near today's Stop 3). The terrace surface is folded and faulted, and reaches a maximum elevation of >200 m at the eastern end of Palliser Bay (Begg and Johnston, 2000). As we drive south, and the road bends right to climb up on to the terrace, the marine interval is well-exposed in a road cut on the left-hand side of the road. Here, Schermer et al. (2009) collected an Optically Stimulated Luminescence sample of sand that yielded an age of 127 ± 10 ka (1 $\sigma$), consistent with the marine unit being deposited during Oxygen Isotope Stage 5e.

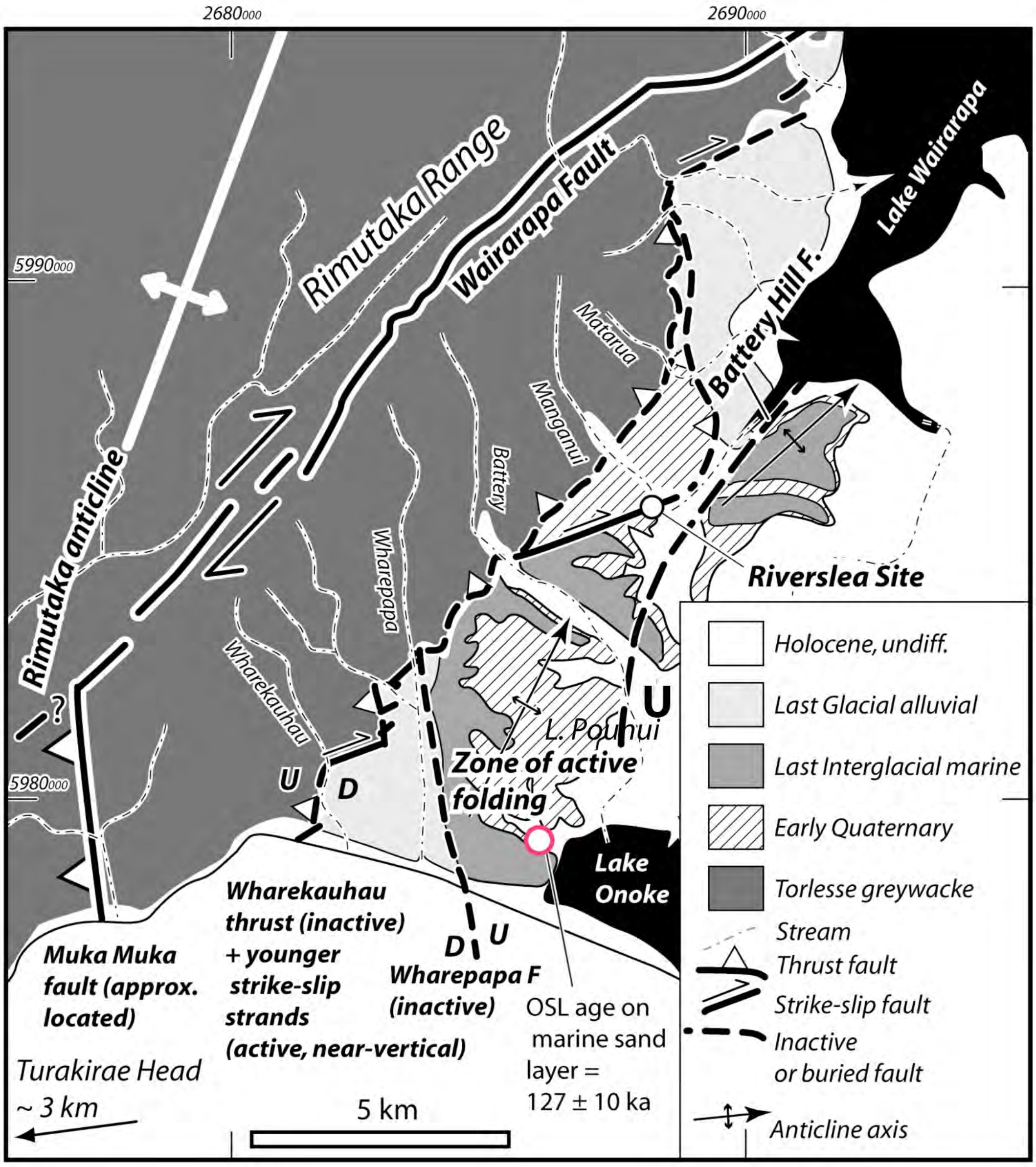


**Figure 11.** Late Quaternary geology, faults and folds at the SW end of the Wairarapa Valley. Red circle shows location of the optional stop.

## STOP 2. Wharekauhau Stream Mouth, Palliser Bay *(Walking circuit).* For location see Figures 12 and 13.

*Park vehicle at mouth of Wharekauhau Stream (do not attempt to cross it in vehicles). Walk upstream, stopping first to look at stratigraphic relations near the mouth of the stream **(Stop 2a)**. Proceed upstream (about 20 minutes) to an exposure of unit 3 **(Stop 2b)** and further upstream to a large exposure of the Wharekauhau thrust **(Stop 2c)**. Return downstream and take the farm track up to the ridgetop (large flat paddock) between Te Mahonge and Wharekauhau Streams **(Stop 2d)**. Walk down the track to Te Mahonge stream to see the Wharekauhau thrust exposed on the track **(Stop 2e)** and the west bank of the stream **(Stop 2f)**. Return along the coast to vehicles. Total time away from vehicles 2-3 hours.*

Travelling west from the optional stop, the road drops below the terrace surface and cuts down through the underlying terrace deposits (Figs. 11 and 13). Along the banks of Wharepapa River, we can see late Quaternary marine sands and gravels near the base of the cliffs, overlain by grey-colored lacustrine silts and alluvial gravels and yellow-weathering, post-last-glacial “Waiohine” gravels at the top of the terrace sequence. Wharepapa Stream, which the road crosses (after a left-hand hair-pin turn) is traversed by a NNW-striking fault that offsets the terrace surface (up to the east) by ~20 m. The western, downthrown side of the fault is infilled and partially buried by the young "Waiohine" gravels (e.g., Kingma, 1967; Rollo 1992; Begg and Mazengarb 1996; McClymont 2000). This near-surface deformation, together with deep incision of the Waiohine surface in this area, is interpreted by Schermer et al., (2009) to reflect deformation in the hangingwall of a blind thrust at depth.

**STOP 2a: Quaternary stratigraphy at Wharekauhau Stream mouth**
*Time at this stop approximately 20 minutes.*

Near the south coast of the Wairarapa Valley, late Quaternary strata and their corresponding landforms, such as wave-cut platforms and fluvial terrace surfaces, record a progression of relative sea level changes, periods of deposition, and pulses of deformation near the Wairarapa fault since ~125 ka. The Wharekauhau thrust separates uplifted Mesozoic greywacke on the northwest from Quaternary strata of the Wairarapa basin on the southeast. Quaternary strata in the footwall of the fault chiefly consist of last interglacial marine deposits and alluvial fan gravels derived from the Rimutaka Range. Partly overlapping the fault, and (as we will argue) post-dating its activity are the post-LGM “Waiohine gravels” (Q2 unit of Begg and Johnston, 2000). To the west of the Wharekauhau thrust, the late Quaternary sequence was deposited unconformably above Mesozoic graywacke, whereas to the east of the thrust, the same strata overlie a substrate of Pliocene-Pleistocene marine to non-marine strata (e.g., Begg and Johnston, 2000). The late Quaternary sequence provides a sensitive geological record of landscape evolution and deformation (including both folding and fault slip). In this region our stratigraphic work built upon that of earlier studies (Eade, 1995; Grapes and Wellman, 1993; Shulmeister & Grapes, 2000; Shulmeister et al., 2000, Marra, 2003). Unit designations used here (Fig. 14) are newly defined and do not necessarily correspond to the (varied) nomenclature used in the earlier work (most of which is unpublished).

## Stop 2 Wharekauhau fault exposures

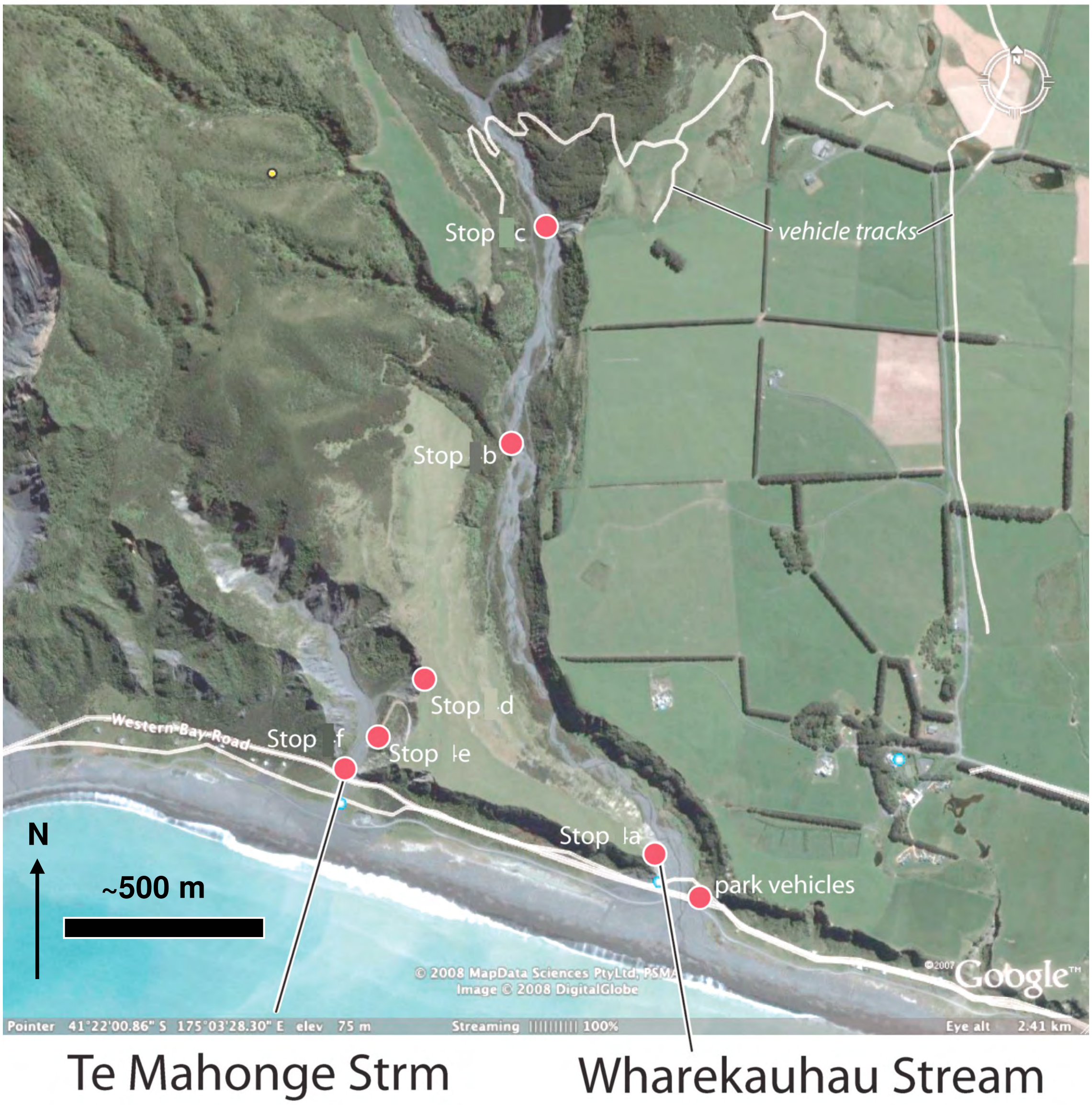


**Figure 12.** Google Earth map of Stop 2 showing round-trip walking route between Wharehauhau and Te Mahonge Streams and sites visited along the trace of the Wharekauhau thrust near the Palliser Bay coast.

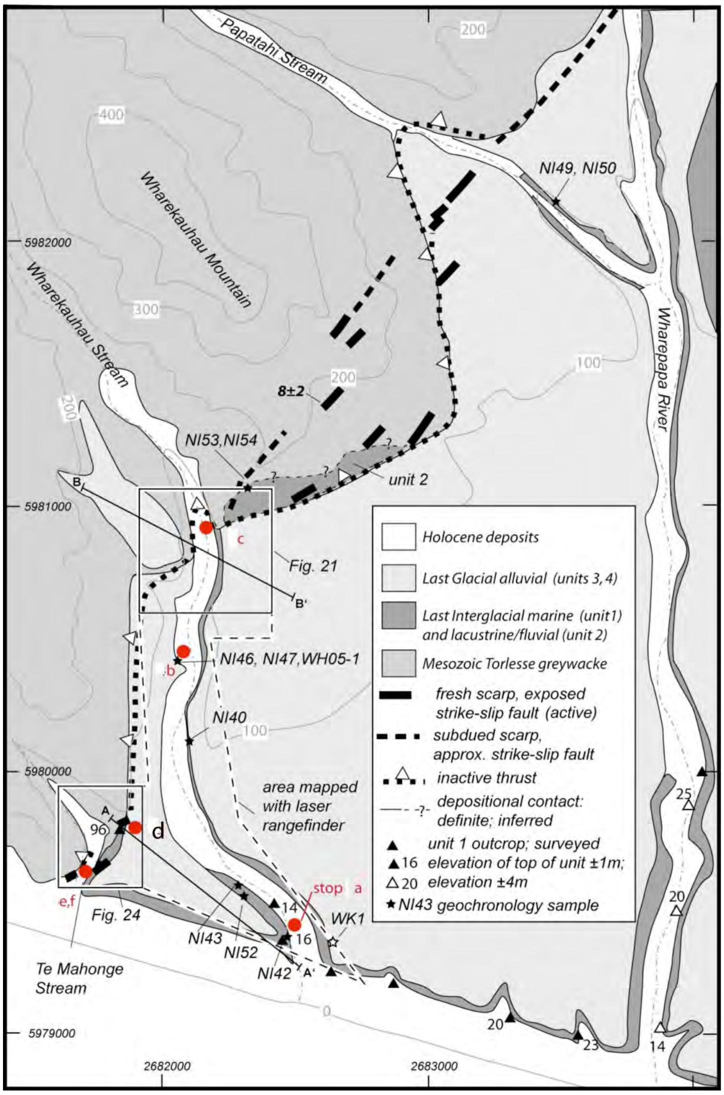

**Figure 13**. Geology of Wharekauhau segment, showing Quaternary unit designations as described in text and Figure 20, fault and fold traces, sample locations, and field trip stops. Open star shows sample location from Wang (2001). Surveyed elevation of the top of unit 1 shallow marine deposits is indicated next to triangles; no outcrops of unit 1 occur north of the northermost symbols. Open triangles indicate locations with elevations that are not controlled by detailed surveying. Dashed outline shows area of detailed mapping and laser surveying, two portions of which are detailed in Figures 21, 24. Location of cross sections A-A' and B-B' are indicated. Topographic contours are in meters; grid marks (in meters) refer to the New Zealand Map Grid Coordinate System.

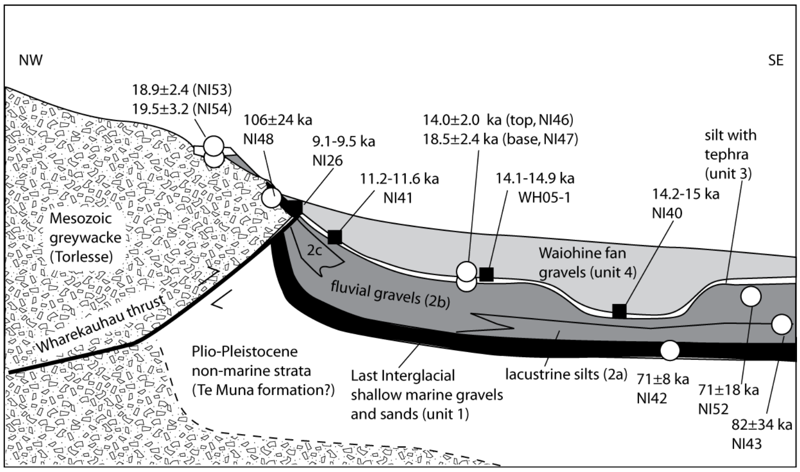


**Figure 14.** Schematic cross section of stratigraphy in the detailed study area of Figure 13. Squares=location of radiocarbon samples (wood from in-situ roots, stumps); circles=location of OSL samples (silts, fine sands). Age ranges for radiocarbon samples are calibrated age range at 95% confidence. Errors on OSL ages are 2σ.

Local exposures of marine sands and gravels (similar to those exposed east of Wharepapa River), herein termed unit 1, occur as a 7-9 m thick sequence in the hangingwall and footwall of the Wharekauhau thrust. In the hangingwall at Te Mahonge Stream, unit 1 overlies greywacke bedrock. In the footwall at the mouth of Wharekauhau Stream (Stop 2a), unit 1 overlies fluvial gravels possibly belonging to the Te Muna Formation (Fig. 14). OSL samples of marine sands collected from unit 1 yielded ages of 106 ±24 ka (NI48) and 71±8 ka (NI42) (2σ errors). As expected, the three samples of marine sands (including the one at the optional stop east of Wharepapa river, which is not in stratigraphic continuity with the fault-proximal marine unit 1) yield ages that are indicative of the last interglacial sea-level highstand (oxygen isotope stage [OIS] 5). The different locations and the higher elevation and older age of the sample east of Wharepapa River (NI51) relative to NI42 (Figs. 11, 13) suggest their deposition during different sea-level high stands (substages) within OIS 5.

In the footwall of the Wharekauhau thrust, the marine gravels are overlain conformably by ~9 m of organic-rich lacustrine mud, silt, and gravelly silt that locally contains tree stumps in growth position (unit 2a). This unit is interpreted to have been deposited during an interglacial climate in an estuarine lagoon similar to present-day Lake Onoke (Eade, 1995; Marra, 2003; Shulmeister et al., 2000). Unit 2a interfingers northward and westward with, grades laterally into, and is overlain by fluvial gravels containing clasts eroded from the Rimutaka Range (unit 2b). Towards the top of unit 2b, gravels have a distinctive yellowish brown color and contain local thin (<0.5m) silt beds with rooted stumps in growth position. Unit 2 coarsens and thickens towards the trace of the Wharekauhau thrust, where we recognize a locally exposed bouldery facies, unit 2c. These coarse gravels interfinger southeastward with better sorted and stratified gravels typical of unit 2b.

Samples from unit 2 yielded OSL ages that are consistent with deposition near the end of the last interglacial at ~80-70ka (i.e., OIS 5a). Sample NI43 from the lower part of unit 2b yielded an age of 82±34 ka (Figs. 19, 20). This sample is located ~4 m above silts of unit 2b dated by OSL at ~115 ±66 ka (Marra, 2003) and ~16m above a sample of unit 2a dated at 117±60 ka (Marra, 2003) (2σ errors). A higher sample from unit 2b, ~20m above sample NI43, yielded an age of of 71±18 ka (sample NI52, Figs. 19, 20). We note that our dating accords with the last-interglacial interpretation of these units by Grapes and Wellman (1993) and Shulmeister et al., (2000) and the interpretations of Marra (2003) based on the fossil insect assemblage in unit 2a.

**STOP 2b: Upper part of Quaternary stratigraphy at Wharekauhau Stream**
*Total time at this stop about 20 minutes.*

At this stop we will see an exposure of the widespread sandy silt (unit 3) up to ~2 m thick that caps the unit 2b gravels, and overlying fluvial gravels (unit 4). At this location, the units appear conformable. Grapes and Wellman (1993) reported that this silt contains shards of the Kawakawa tephra (26,500 calib yr B.P; (Wilson et al., 1988) and abundant *in-situ* stumps and roots at its top dated at 12,450 ± 120 and 12,760 ± 110 $^{14}$C yr BP (Grapes and Wellman, 1993) (these correspond to calibrated ages of ~15 ka).

Grapes and Wellman (1993) interpreted the silt as a loess deposited on an abandoned fan surface, but the local presence of poorly sorted fine pebbles in the unit led Shulmeister et al., (2000) to reinterpret the unit as an overbank deposit mixed with loess. Our new OSL ages from samples near the base of the unit are 18.5 ± 2.4 ka and 19.5 ± 3.2 ka (Fig. 14). $^{14}C$ samples from the top of unit 3 range from 15 ka to ~9ka, with age decreasing northward and with elevation (Fig. 20). As we will see at later stops, there is a marked angular unconformity beneath unit 3. Furthermore, unit 3 mantles a topographical paleoscarp created by slip on the Wharekauhau thrust, and thus appears to be wind-deposited (a loess). The data suggest that the silt of unit 3 and overlying gravels of unit 4 onlapped northward across the scarp over a period of >5,000 years.

Unit 3 is overlain by alluvial fan gravels (unit 4) that are topped by the terrace tread referred to as the “Waiohine” surface by Grapes and Wellman (1993). Wang (2001) reported a ~5 ka OSL age on a silt lens collected 0.6 m beneath this surface near Stop 2a (sample WK-1).

**STOP 2c: Wharekauhau thrust exposure at Wharekauhau Stream**

*Discuss the evidence for thrusting and abandonment of the thrust. Total time at this stop about 60 minutes.*

At this exposure we can see the imbricate nature of the Wharekauhau thrust as well as key stratigraphic relationships that constrain its timing (Figs. 21, 22). On the right-hand side of the exposure there is evidence of two distinct periods of unit 2b deposition, separated by a soft, red-brown gravelly clay that we interpret as a paleosol. Unit 2c, consisting of disorganized and bouldery, angular gravels, is only found above this clay, and interfingers southward with fluvial gravels of the upper part of unit 2b. Across the length of the exposure, unit 2c occurs in fault contact beneath a lower imbricate of the Wharekauhau thrust, while at the southern end, it is also in discordant depositional contact against steeply dipping (beach) strata of unit 1 in the main hangingwall of the thrust (somewhat obscured by flax bushes). We interpret this discordant contact as a buttress unconformity and unit 2c to represent colluvium derived from the emergent thrust scarp. Older parts of unit 2c were overthrust during fault slip, while younger parts were deposited against the emergent hangingwall, partially burying it. In the upper parts of this exposure, it can be seen that units 3 and 4 overlap the Wharekauhau thrust and units 1 and 2 along an angular unconformity. In the hangingwall of the thrust above the north end of the outcrop, unit 3 occurs as a 5-6 m-thick massive silt that is not

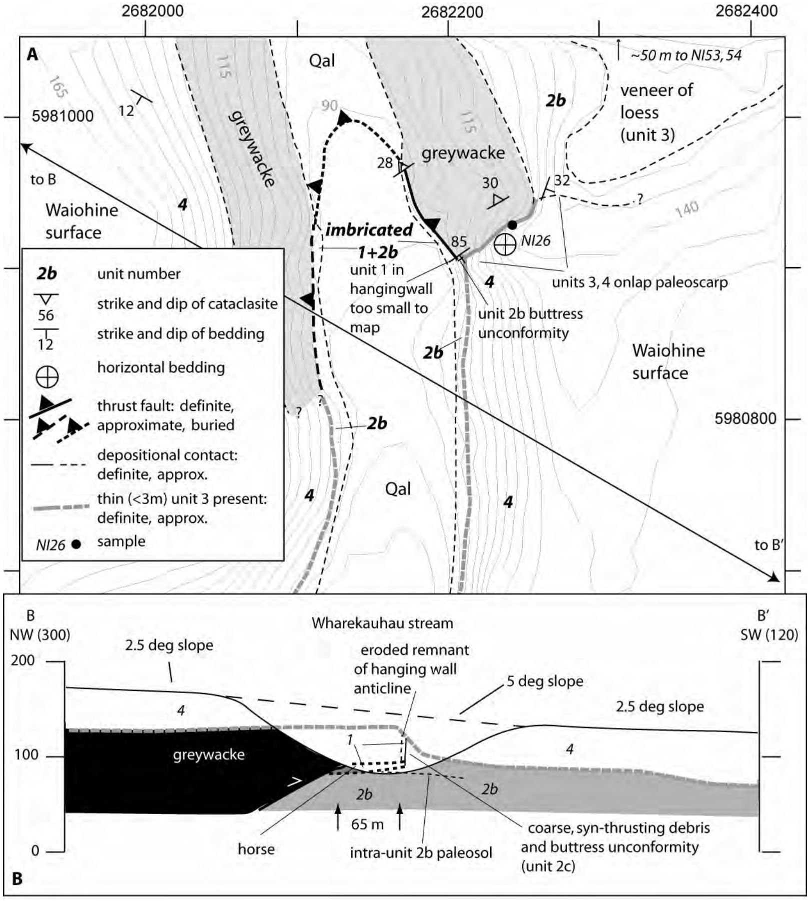


**Figure 21**. a) Detailed map of Wharekauhau stream area (Stop 4c) derived from surveying topography and geologic contacts with a laser rangefinder. Locations of geochronological samples shown with black dots. b) Cross section B-B', no vertical exaggeration constructed perpendicular to a thrust strike of 210 (N30E) consistent with the structure contours drawn across Wharekauhau stream and the regional trend of the fault. Location shown on Figure 19. Fine dashed lines show bedding traces.

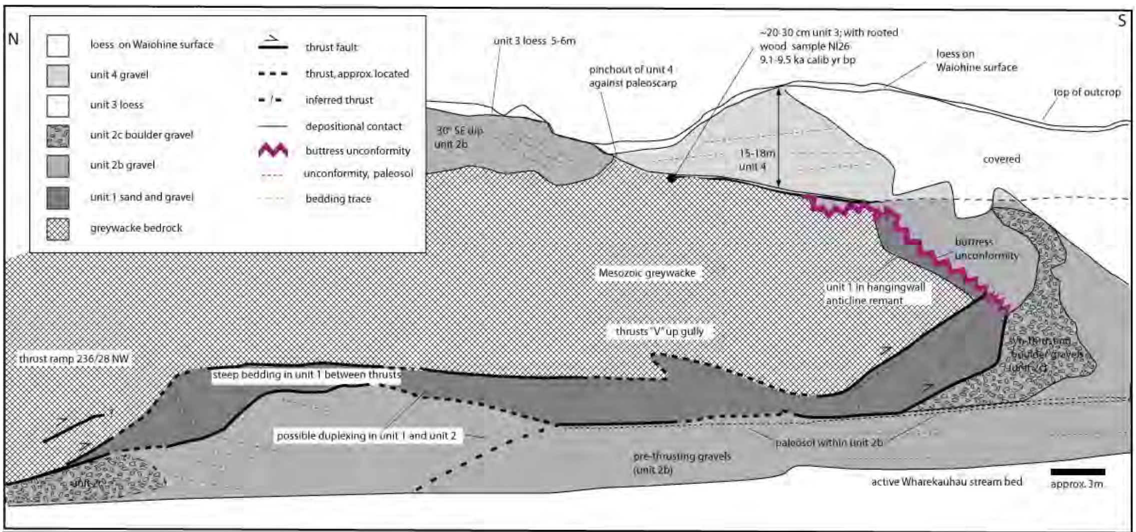


**Figure 22.** Tracing of a photograph of an outcrop of the thrust at stop 4c. Duplexing in unit 2b is inferred from discontinuities in bedding; duplexing in unit 1 is inferred from extreme thickening of unit in horse relative to undeformed exposures.

capped by any unit 4 gravels. About 20 m to the southeast, unit 3 continues as a <0.5m thick layer that is overlain by unit 4. This fault-proximal part of unit 3 appears to mantle a paleoscarp formed in older units. The angular discordance between unit 3 and older Quaternary strata is typically ~30° here (Fig. 21), but disappears to the south (e.g., stop 4b).

Structural features are also well displayed at this outcrop, where the Wharekauhau thrust consists of two subparallel thrust planes that are spaced ~1-1.5 m apart, and that flatten from ~30°NW dip to horizontal towards the south (Fig. 22). The higher thrust juxtaposes highly fractured Cretaceous Torlesse greywacke (foliated cataclasite) in its hangingwall to the northwest above steeply dipping unit 1 strata to the southeast. The lower thrust juxtaposes unit 1 beach gravels above gently dipping strata of unit 2 (subunits 2b and 2c). Between the two fault planes, the slice of steeply dipping strata of unit 1 occurs as a "horse" that is internally folded. The structural thickness of unit 1 in this horse (up to ~100m) is > 10 times greater than the observed maximum stratigraphic thickness of unit 1 away from the fault (7-9 m). Although the discontinuity of exposure prevents us from verifying the inference, this relationship suggests that unit 1 in the horse is repeated several times by thrust duplexing or distributed deformation. Imbricate thrusts may also occur within unit 2 beneath the lower thrust.

The geometric and stratigraphic relationships suggest initital formation of a fault-propagation fold, followed by the fault tip propagating upward to the surface, and cutting off the steep forelimb. The subvertical dips in the imbricate fault slice of unit 1 and locally in unit 2 immediately below the lower thrust and in unit 1 above the upper thrust indicate that the strata were folded prior to thrusting. The eastward shallowing of the thrust planes, and the coincidence of the flat thrust surface with the paleosol within unit 2b (Fig. 22) suggests that the thrust ramped upward to the contemporary free surface before collapsing gravitationally.

In Wharekauhau Stream, corresponding hangingwall and footwall cutoffs are not exposed so there is little control on total shortening. Cross section B-B' can be used, however, to calculate a minimum heave of 65 ±2m on the upper thrust of the imbricate system from the amount of overlap of the greywacke and the fragment of unit 1 in the hangingwall, assuming a thrust strike of N30E (Fig. 21b). Doubling that to account for the similar overlap of unit 1 on the lower fault (and without accounting for any duplexing) gives a minimum of 130 m shortening across both thrusts. Varying the strike of the thrust to account for poor exposure of the surface results in <15m difference in the heave.

**STOP 2d: Deformation (?) of the Waiohine surface at Te Mahonge Stream**
*Return downstream and take the track up to the paddock between Te Mahonge and Wharekauhau Streams. View and discuss the (lack of) evidence for 1855 surface rupture on the paddock surface, and the stratigraphy exposed in the slip face. Total time at this stop about 40 minutes (including the walk).*

"Te Mangonge" Stream is an historic locality, described by Rodney Grapes in his book, *"Magnitude 8 Plus*" as the location where, immediately after the 1855 earthquake, Edward Roberts, a surveyor for the *Royal Engineers and Clerk for Works,* observed a break along the creek, across which "the range of hills [Rimutaka Range] have gone up alone forming a perpendicular precipice." As a consequence of this uplift of the coastal rock platform, a coastal route negotiable by foot or ox-cart (or mountain bike) was opened up for the first time between the Wairarapa and Wellington. Charles Lyell met Roberts in England a year later, and included the surveyor's account of 1855 co-seismic deformation into his book, "*Principals of Geology"* (Lyell, 1868), along with a cross-section of the "fault and fissure" in "Te Mangonge" Stream (Fig. 23a). The maximum coastal uplift in 1855 occurred ~4 km to the northeast of Turakirae Head, where the 1855 beach ridge was elevated vertically by 6.4 m on the upper block of the Wharekauhau Thrust (Hull and McSaveney, 1996; McSaveney et al., 2006).

A review of the historical record (Downes and Grapes, 1999; Ongley, 1943) indicates that there was no definitive report on the nature of any earthquake rupture at the coast in 1855 at either Te Mahonge or Wharekauhau streams. The report that Edward Roberts gave to Lyell does not describe the location of the "precipice". Later interviews of Roberts by Lyell state that Roberts found "raised nullipores" 9 feet above the tide line the morning after the 1855 earthquake near Muka Muka rocks (Lyell, 1868). Although the exact location of his observation is uncertain, Muka Muka rocks is west of the NW corner of Palliser Bay and ~3 km west of Te Mahonge stream. This is evidence of coseismic coastal uplift relative to sea level, but it is not evidence for a rupture plane in Te Mahonge stream.

The diagram published by Lyell (1868) (Fig. 24a) showing the fault that he inferred to have slipped in 1855 actually came from a description provided by Walter Mantell, a geologist who was in New Zealand at the time of the earthquake:

> *"According to Mr. Mantell the risen mass consists of old stratified argillites, with the normal composition of argillaceous schists, but without schistosity. This mass forms a several hundred foot high cliff towards the sea, whereas the tertiary marine strata, which are exposed to the east, next to the shore, form another relatively low cliff which would not be higher than eighty feet. These tertiary strata did not rise." (Lyell, 1856), as translated in Downes and Grapes, 1999)*

The juxtaposition of "old argillite" (greywacke) against "Tertiary strata" (Quaternary silts and gravels) describes the relationships near the mouth of Te Mahonge stream (stops 4e, 4f) but is not, however, the same place as where Roberts measured the "raised nullipores", nor is it a description of a coseismic rupture or scarp.

In 1934-35 M. Ongley (1943) mapped scarps along the 1855 rupture from Alfredton to the coast. He disagreed with Lyell on several points, noting that the fault that Mantell described was not at the NW corner of Palliser Bay as originally described, but was further east (at Te Mahonge stream). He also noted the fault is not a vertical fissure as reported in Lyell (1868), but a gently dipping thrust. Furthermore, Ongley (1943) did not find a surface scarp on either side of Wharekauhau stream, and stated that the southernmost scarp was located ~1mile (1.6 km) north of the coast (on the SE flank of Wharekauhau Mountain). The scarps that he illustrates (Figs 1, 2 in Ongley, 1943) trend more easterly than the thrust contact and may be some of the strike-slip features or landslide scarps mapped by Schermer et al. (2009). Ongley (1943) stated that *"the line of it [the 1855 scarp] runs to the coast well west of the fault between the two formations"*. Furthermore, although Ongley (1943) shows a dashed line of surface

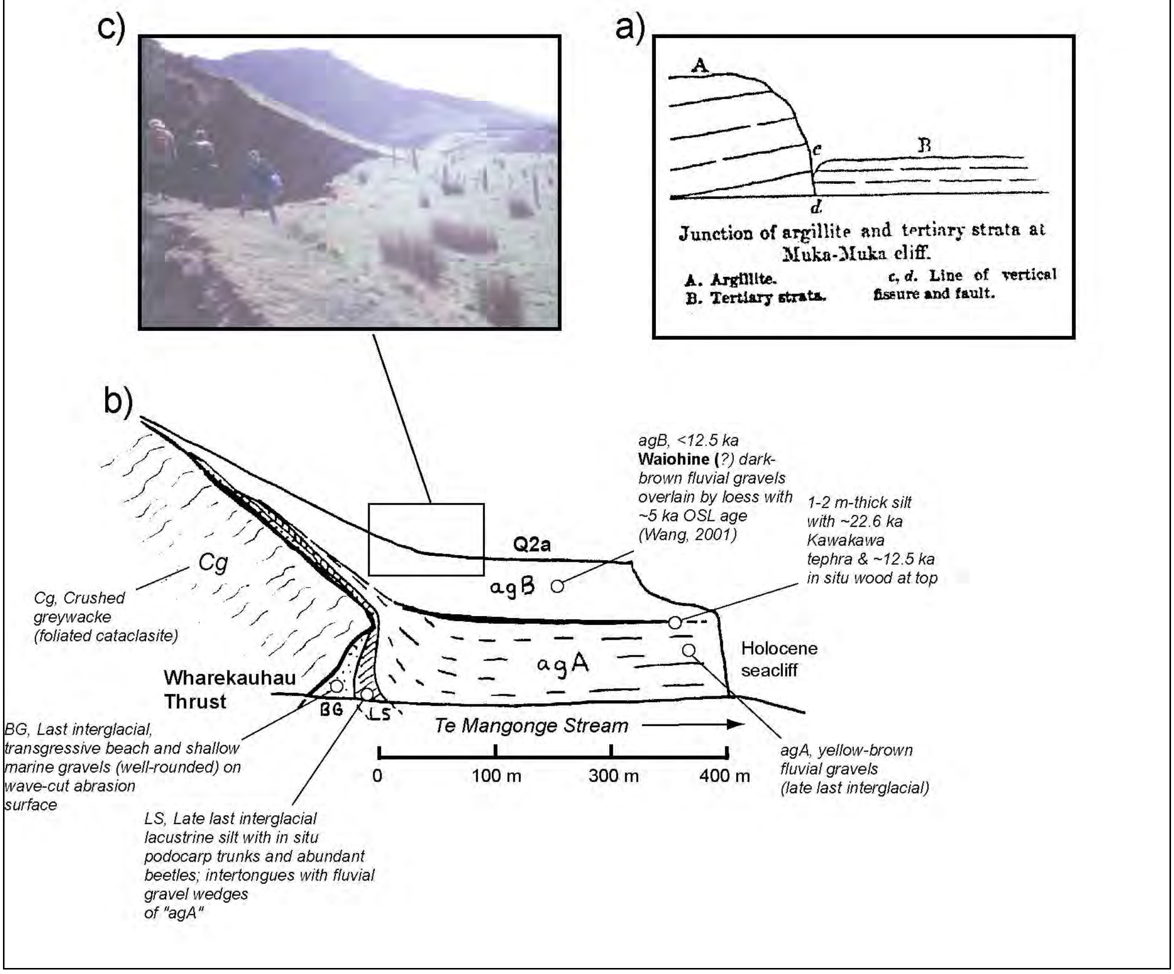


**Figure 23.** Previous interpretations of the Wharekauhau thrust as exposed in Te Mahonge and Wharekauhau Streams near the Palliser Bay coast. a) diagram of Te Mahonge Stream exposure of the fault (illustration in Lyell, 1868; note the steep dip of the fault); b) diagram after Grapes and Wellman (1993) who interpreted the Waiohine Terrace surface as being deformed and tilted across the fault at the location of photograph (c), Note that the top of Grapes and Wellman's "agB" unit is equivalent to the unit "Q2a" of Begg and Johnston (2000), and to the top of "unit 4" of Schermer et al. (2009, as used in this guide).

ruptures on his map south of Lake Wairarapa, none of the area traversed for the present study has definite fault scarps that are as steep or fresh-looking as the area to the north from Hinaburn to Alfredton (e.g. Grapes and Wellman, 1988; Rodgers and Little, 2006; Schermer et al., 2004). Although Ongley (1943) stated clearly that Lyell's diagram did not represent the 1855 rupture, the error has persisted through recent publications (Grapes and Downes, 1997; Grapes and Wellman, 1993; Sibson, 2006).

The location of Roberts' coastal uplift observation on Palliser Bay is constrained by the beach profiles of Hull and McSaveney, (1996); McSaveney et al., (2006) who show that the easternmost preserved uplifted beach ridge is <1km east of Muka Muka stream (Fig 13) and interpret this to be approximately the location of Roberts' observation in 1855. Given the evidence for lack of recent rupture of the Wharekauhau thrust, we suggest that the fault, if indeed it ruptured the surface at the coast, did so closer to Muka Muka stream. McSaveny et al (2006) reach a similar conclusion from their detailed analysis of the Turakirae head data.

At this stop (Fig. 23c), vertically above the exposures of the thrust in Te Mahonge Stream, the Waiohine terrace surface was interpreted by Grapes and Wellman (1993) to be warped upward during rupture of the Wharekauhau thrust in 1855 and prior earthquakes. Our new mapping shows that the Waiohine gravels (unit 4) do not show the same dip as the terrace surface, which is mantled by a younger layer of colluvium derived from the hilly topography northwest of the inactive thrust trace. The strata in unit 4 everywhere dip <15° and onlap depositionally against the more steeply dipping strata in the thrust hangingwall (Fig. 24). From these relationships we infer that the Waiohine surface at the top of unit 4 is undeformed and that the local increase in surface slope of the hillside adjacent to the paleoscarp is a primary depositional feature of the landscape (slope colluvium) and not the result of tectonic deformation in 1855 or at any earlier time.

Looking back towards stop 4c, the Waiohine surface is visible in both the hangingwall and footwall of the thrust as the cleared paddocks, but it is not continuous across Wharekauhau stream (Fig. 21b). Grapes and Wellman (1993) inferred that ~20 m of height difference between these two parts of the surface was due to deformation along the thrust. A laser-surveyed topographic profile along the Waiohine surface across the trace of the thrust from NW to SE across the stream shows the surface is 15 m lower on the SE side of the stream, but the dips are low (2.5-5°) and it is not clear if there is a change in dip that can be associated with the trace of the thrust (Fig. 21b). We interpret the dips as primary features of the fan surface. If the change in slope is indeed due to thrusting, the active fault must lie below the surface, and can not have the same near-surface expression as the (inactive) Wharekauhau thrust.

**STOP 2e: Wharekauhau thrust at Te Mahonge Stream**

*Walk down the farm track to the exposure of the thrust at the base of the track (true left bank of the stream). Total time at this stop about 40 minutes (including the walk).*

At this location we can see the two thrusts enclosing the horse of unit 1, and higher on the slope, the unconformity between unit 2, which dips 25-90°, and units 3 and 4, which dip ~10° (Figs. 24d, 25). If there is time to walk upstream to view a large exposure in the slip face, we will see unit 4 onlapping the paleoscarp (Figs. 24a, b).

The two thrusts flatten in an eastward direction from NW dipping to subhorizontal (Fig. 24b). On the west bank of Te Mahonge Stream (stop 4f), both thrusts are steeply dipping. Here, the upper thrust is subhorizontal and the lower thrust is oriented 358/16E. Cataclasite fabric in the hangingwall greywacke also flattens upward, from 68°NW to 23°NW, with the hinge direction of this antiform trending 026 (Fig. 24c). Within the horse, unit 1 is folded by "drag" on the upper thrust (Fig. 25).

Above the thrust, a hangingwall anticline deforms the greywacke and the unconformably overlying units 1 and 2. Near the crest of the anticline (near the top of the track, and a few meters up from the base of the track), several steeply SE- and NW-dipping faults with <0.5m normal separation cut unit 2, perhaps to accommodate localized extension above the fold crest. Units 3 and 4 onlap, pinch out against, and partially bury, a paleoscarp defined by the older, more strongly deformed hangingwall units (Fig. 25).

In all locations strata at the top of unit 2 have a similar dip to those at the bottom of that unit and to beds in unit 1 (Fig. 24d). This concordance indicates no measurable tilting during sedimentation of units 1 and 2, although the variability of dips, the sparsity of data near the top of the unit, and the difficulty of measuring bedding in coarse fan gravels could allow for some minor (<5°) shallowing upsection.

The map pattern and thickness variations of units 3 and 4 seen here and in Wharekauhau stream indicate that deposition of these units was strongly influenced by an earlier scarp generated along the Wharekauhau thrust. The angular unconformity beneath these two units, their overlapping of the thrust, and their subhorizontal attitude indicates the thrust was not active at the time of deposition (or subsequently).

Structural evidence exists for steeply dipping faults that post-date motion on the Wharekauhau thrust. Although we have not found a continous, throughgoing fault, several map- and outcrop-scale observations support the hypothesis of late strike-slip faulting that occurs in the vicinity of the inactive thrust traces. The most compelling evidence comes from our detailed mapping. Structure contours drawn parallel to strike from surveyed elevations on the fault surface indicate that the thrust surfaces in Te Mahonge and Wharekauhau stream are not coplanar, and further show that the outcrop in Te Mahonge Stream has been folded or faulted to lower elevation than that in Wharekauhau Stream. However, since the thrust at both locations shows the same flattening-upward geometry (Figs. 21b, 24b), and similar strike and dip of the thrust, fault displacement appears more likely than folding.

In outcrop, exposures in Te Mahonge Stream suggest that following erosion of the thrust and deposition of unit 3, several steeply dipping strike-slip(?) faults cut through the Quaternary units (Figs. 24, 25). Just south of the thrust exposure on the east side of the stream, a fault oriented ~075/80SE causes ~3m of down to the southeast vertical separation of the contact between units 2 and 3. Cross section relations implied by the fold geometry in unit 2 suggest that the separation on the unit 1-unit 2 contact is up to the southeast (Fig. 24b). Because the two contacts are not parallel, the opposite vertical separations can be most simply explained by dextral slip. We also interpret this fault to extend across the stream to the west, where the lower “thrust” has been reoriented to a vertical dip. This fault does not cut up to the Waiohine surface. Several steep faults are also observed cutting hangingwall strata in the slip face exposure to the north of this stop, but most are too small to show on the map (Fig. 24a). These faults are NE-striking, steeply dipping faults with at most a few meters of vertical and horizontal separation (Fig. 24e). The exposed faults locally cut up into the upper part of unit 4 but do not cut the Waiohine surface. The presence of both reverse and normal separations suggests strike-slip faulting, but subhorizontal slickenlines were found only on one fault.

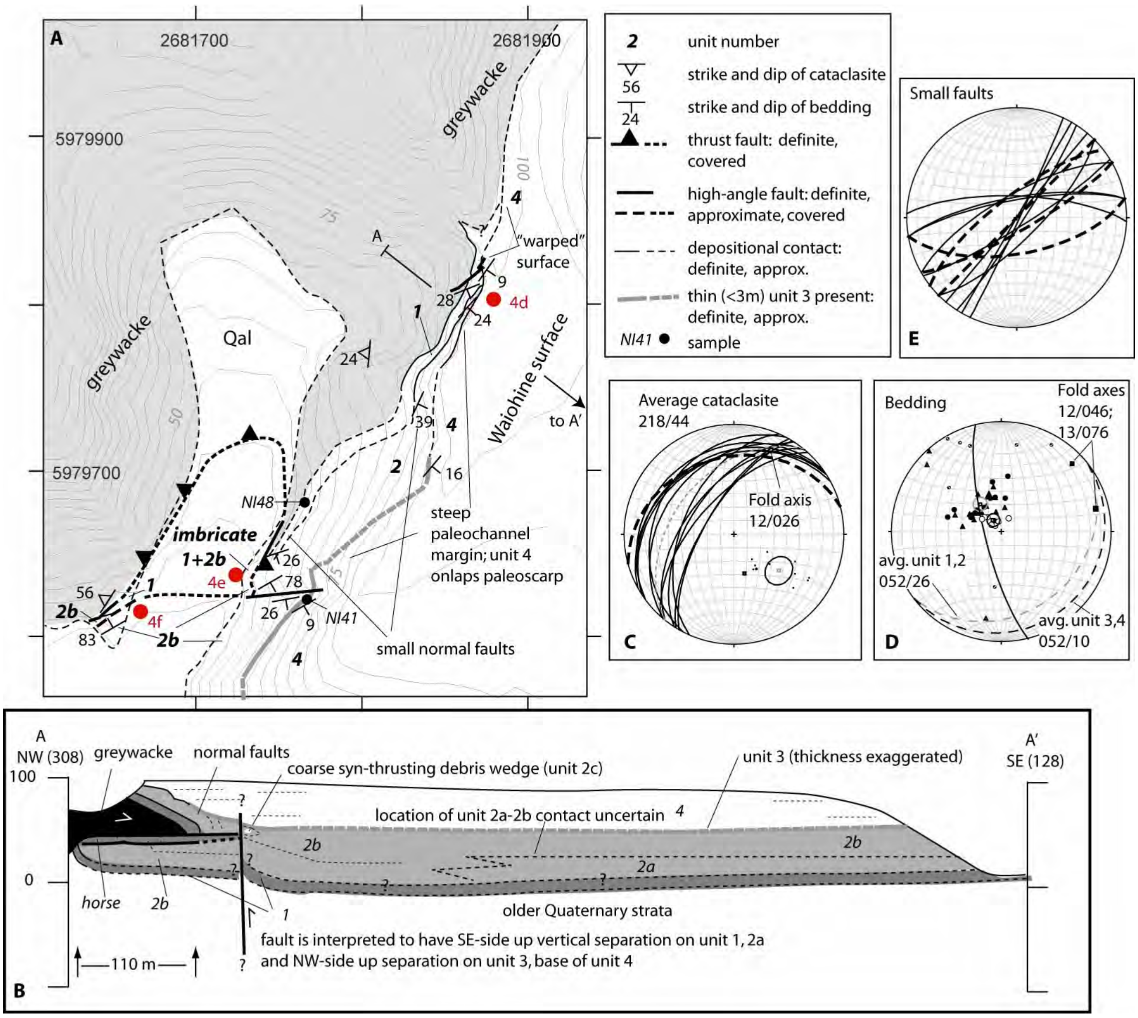


**Figure 24**. a) Detailed map of Te Mahonge stream area (stops 2d, 2e, 2f) derived from surveying topography and geologic contacts with a laser rangefinder. Contour interval is 5m. b) Cross section A-A' (location on Fig. 19), no vertical exaggeration, constructed perpendicular to the average cataclasite strike of 218 (N38E). Fine dashed lines show bedding traces. c) Equal-area stereoplot of structures related to Wharekauhau thrust. Black great circles are cataclasized greywacke planes, with poles shown as dots; black dashed line is minor thrust plane (60 cm separation); grey dotted line is mean plane, with mean pole and cone of confidence shown in open square and circle, respectively. Calculated fold axis assumes scatter of planes is due to upward flattening of the thrust. d) Equal-area stereoplot of poles to bedding: triangles-unit 1; filled-unit 2; open circles units 3, 4. Fold axis of all unit 1 and 2 data shown in black square (13/076) and best-fit great circle, other black square is small-scale fold in duplex. Excluding steep beds in duplex and adjacent to thrust (smaller symbols), average orientations were calculated for bedding in hangingwall and footwall: Mean vector and plane for units 1 and 2 shown by grey cone of confidence and dashed great circle; mean vector and plane for units 3 and 4 shown by black cone of confidence and dashed great circle. e) Stereoplot of small-scale faults adjacent to thrust. Solid great circles are normal faults cutting units 1 and 2 at crest of hangingwall anticline, dashed great circles are inferred strike-slip faults that cut up into units 3 and 4.

## STOP 2e: Wharekauhau thrust at Te Mahonge Stream

*Walk across the stream to the true right bank. Total time at this stop about 20 minutes.*

At this location we can see the steeper portions of the two thrusts enclosing the horse of unit 1, the unit 1-unit 2 contact within the horse, and the steeply dipping bedding in the footwall of the lower thrust (Fig. 24). Greywacke cataclasite is also well exposed. Relations at Te Mahonge stream provide constraints on the geometry of the thrust-related deformation, and minimum shortening and slip rates along the thrust. We will summarise these relations at this stop.

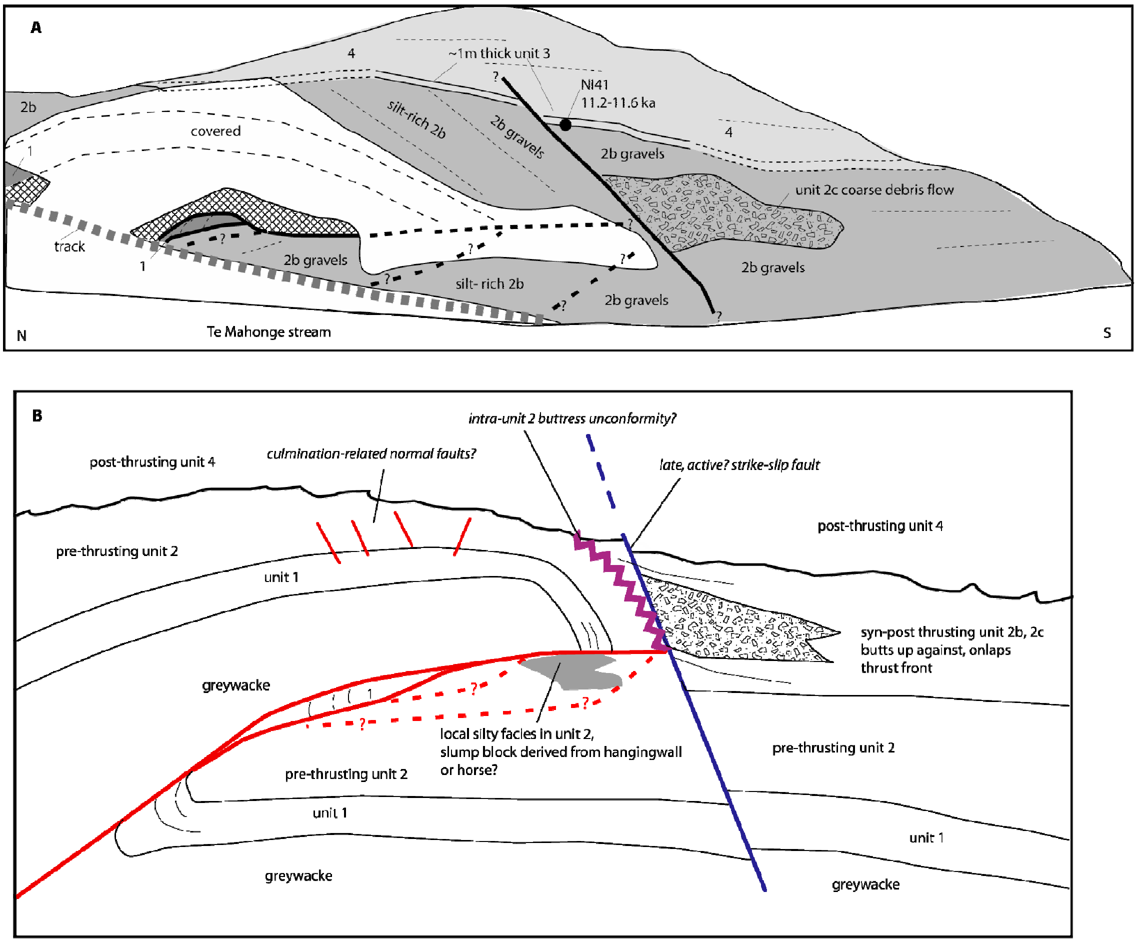


**Figure 25**. a) Tracing of a photograph of an outcrop of the thrust at stop 4e. b) Interpretation of fold and thrust geometry in Te Mahonge stream, including data from area to north of stop 4e.

## Summary of magnitude and timing of thrusting on the Wharekauhau thrust

No slickenlines were observed on the thrust plane, so we assume purely dip-slip displacement to calculate a minimum amount of horizontal shortening required by the cross sections. The cross section in Te Mahonge Stream provides a better estimate of slip magnitude because the hangingwall cutoffs of the contacts between greywacke, unit 1, and unit 2 are exposed on the east side of the stream and and the cutoff of the stratigraphic contact between units 1 and 2 within the horse is exposed on the west side of the stream (Fig. 24a), so both could be accurately mapped. Reconstruction of cross sections from Te Mahonge stream (e.g., A-A', Fig. 24b) using the observed range of strikes of contacts and faults yielded a minimum shortening estimate (folding + faulting) of 280±60m.

The vertical component of thrusting (throw) is constrained by the elevation difference between the hangingwall and footwall strata. The throw on the unit 1/unit 2 contact is constrained to 97-102 m. This is a minimum value because the contact is likely folded to lower elevations in the footwall and higher elevations in the hangingwall than the present exposures.

The structural and stratigraphic relationships lead us to infer that the major period of shortening on the Wharekauhau thrust began at ~70 ka. Evidence for the age of initiation of the thrust comes from the observation that bedding in units 1 and 2 is parallel at all locations where we could measure it (Fig. 24d). Although there may have been thrust activity prior to the deposition of unit 1, and/or during the deposition of unit 2b, to cause some (unrecognized) minor fanning of dips within that unit, we infer that deformation of the conformable unit 1-unit 2a contact did not begin until after deposition of the latter. The age of this contact, based on the OSL data described above, is constrained to the interval 106± 24 to 71 ± 8 ka. If we are correct in our inference that thrusting began during deposition of the syntectonic unit 2b, then the OSL data would indicate a thrust initiation age of no older than 71±8 ka.

The evidence further suggests the abandonment of thrusting by ~20 ka. Onlap of the paleoscarp by units 3 and 4 and the angular unconformity at the base of unit 3 suggest that the thrust was inactive at this time. The recognition of a buttress unconformity within unit 2b suggests deposition of that unit took place during the waning stages of thrust activity. Above the angular unconformity, dates on unit 3 nearest the thrust suggest abandonment occurred after 19.5±3.2 to 9.1-9.5 ka (Fig. 20). Two locations at the base of unit 3 are dated by OSL at ~18-20 ka (samples NI54, NI47, Fig. 20), but these occur at sites where there is no clear angular relationship between unit 2 and unit 3. At the place where the angular unconformity is best documented, where unit 3 lies above deformed unit 2b strata in the footwall, wood at the top of unit 3 (Sample NI41) yielded a $^{14}C$ age of 11.2-11.6 ka; however, the base of the unit is not dated at that location. At the only location where the sampled unit 3 overlaps the thrust (NI26), the top of the unit is 9.1-9.5 ka (Fig. 6). The sedimentological characteristics of unit 3 (i.e., very fine-grained, and of uniform thickness to within ~20 m southeast of the thrust) suggest that the thrust was not active during any part of its deposition (e.g., in stark contrast to units 2b, 2c). From these data we infer that the thrust was certainly abandoned by ~9 ka, and more likely was abandoned prior to ~20 ka.

**Vertical and horizontal components of slip rate**

Our new structural and geochronological data provide estimates of the late Quaternary slip rate of the Wharekauhau thrust. These rates are minima because the amount of heave and throw are minimum values and because the age of the top of unit 2b could be younger than our youngest dated sample. From the range of horizontal shortening estimates at Te Mahonge Stream (280±60 m) on the unit 1/unit 2 contact, and given the conservative estimate of the duration of thrusting (106±18 ka to 9.1-9.5 ka), the minimum shortening rate is 1.8-4.7 mm/yr. Using our preferred duration estimate of 71±8 ka to 19.5±3.2 ka results in rate of 3.5-8.4 mm/yr. The vertical component of slip rate (throw rate) due to the Wharekauhau thrust can also be constrained using the minimum throw of 92-102m. Using the conservative estimate of thrusting duration, we estimate a minimum vertical throw rate on the Wharekauhau thrust of 0.8-1.4 mm/yr. Using the preferred timing constraints, the minimum throw rate is 1.5-2.7 mm/yr.

The inferred shortening rate during its activity, 3.5-8.4 mm/yr, exceeds that of all other active thrusts and oblique thrusts in the Hikurangi margin and may have accounted for 11-30% of the margin-normal component of plate motion. After abandonment, deformation at shallow levels has occurred primarily on a segmented fault system that accommodates little to no shortening (<1mm/yr). We infer that present-day deformation (including during 1855) at the southern end of the Wairarapa Fault zone is partitioned between slip on: 1) the more western Wairarapa-Muka Muka fault system (dominantly dextral-slip, but also causing local uplift of the coast near Turakirae Head; 2) a series of discontinuously expressed, near-vertical strike-slip faults and linking blind oblique-reverse thrusts near the trace of the older (inactive) Wharekauhau thrust; and 3) a possible blind thrust fault between Lake Onoke and the western margin of the Wairarapa Valley. The spatial and temporal complexity of the Wharekauhau fault system and the importance it has had in accommodating upper plate deformation argue for an unsteady linkage between upper plate faults and between these faults and the plate interface.

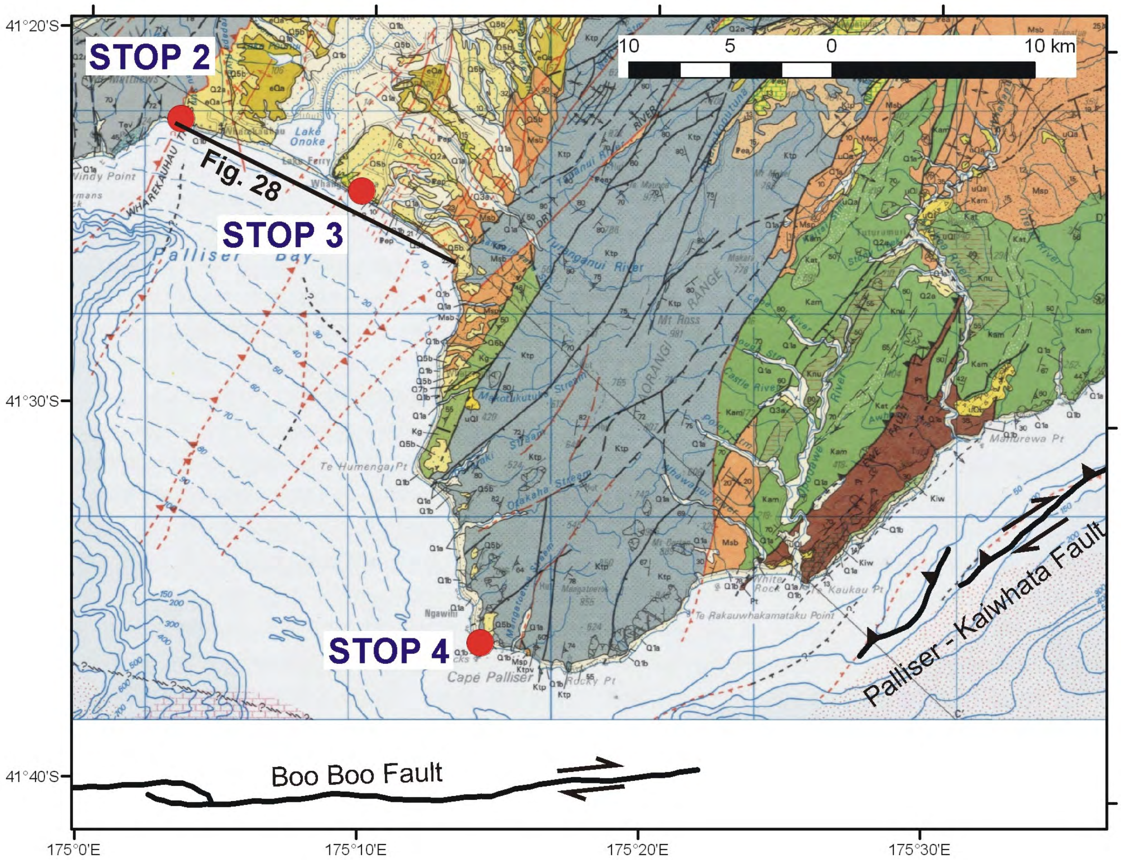


**Figure 26**. Geological map of the Palliser Bay – Cape Palliser area (from Begg & Johnston, 2000). Note the Pleistocene marine terraces (yellow, Q5b) which are semi-continuous between stops 2 and 4. Also shown are major offshore faults (P. Barnes, NIWA, unpublished data), the dextral strike-slip BooBoo Fault and the oblique-dextral Palliser-Kaiwhata Fault.

**STOP 3. Pleistocene marine terrace exposure, Whangaimoana Beach** *(east of Lake Ferry).* **For location see Figures 12 and 13.**

*Access to this stop is across private land (Kaiwaru Station). Park vehicle at fence and walk (carefully) to the edge of the marine terrace. Total time away from vehicles 40 mins.*

The east side of the lower Wairarapa valley (east of Lake Onoke) is, like the west side, characterised by a sequence of uplifted Pleistocene marine terraces overlain by alluvial (mainly fan) deposits (Fig. 26). The marine terraces were studied by Ghani (1978), who interpreted four last interglacial age terraces (80, 84, 100, and 125 ka), but subsequent studies (A. Palmer pers. comm. 2005; J. Begg, pers. comm. 2008) have suggested that some of these ages are likely to be incorrect. Ghani (1978) also interpreted a complex set of faults and folds crossing these terraces (many are shown on Fig. 26), but these were inferred from changes in terrace surface altitudes, which include variable thicknesses of alluvial fan cover, and so do not provide a flat datum for measuring deformation.

A new phase of work is currently being undertaken by Dee Ninis (PhD student, VUW) to date the marine terraces using OSL dating, and to survey the wave cut platform (strath) altitudes using RTK GPS. By collecting these data here and at other sites along a transect along the south Wellington-Wairarapa coast, we will gain a better understanding of the wavelength and mechanisms of uplift in the southern Hikurangi Margin.

Stop 3 is a stream gully exposure through the terrace deposits (Fig. 27) along the coastal cliff 1.6 km southeast of Lake Ferry. The exposure shows a strath cut into blue-grey mudstone bedrock (Late Pliocene Onoke Group), overlain by 7-8 m of interbedded beach gravel and sand. The marine deposits are in turn overlain by 5-6 m of non-marine cover beds - alluvial (river?) gravel and loess. These deposits are fairly typical of the terraces along the Palliser Bay coast, although the beach deposits do vary from being gravel-dominated to sand-dominated and the alluvial deposits vary in thickness significantly.

An OSL sample is currently being processed from this site, but an OSL age of beach sands from a coastal cliff site ~2.5 km to the southeast suggests the terrace probably formed during either the 105 or 125 ka sea level highstand of the last interglacial period. We tentatively favour 125 ka because globally this is marked by a prominent terrace, formed when sea level was 4-6 m above the current level. A minimum altitude of 37 m (a minimum because it is measured at the present day cliff, not the paleo-cliff, which is further inland) indicates a minimum uplift rate of 0.3 mm/yr (37-5 m/125 kyr). The question to be explored from this point on is what is the uplift mechanism?


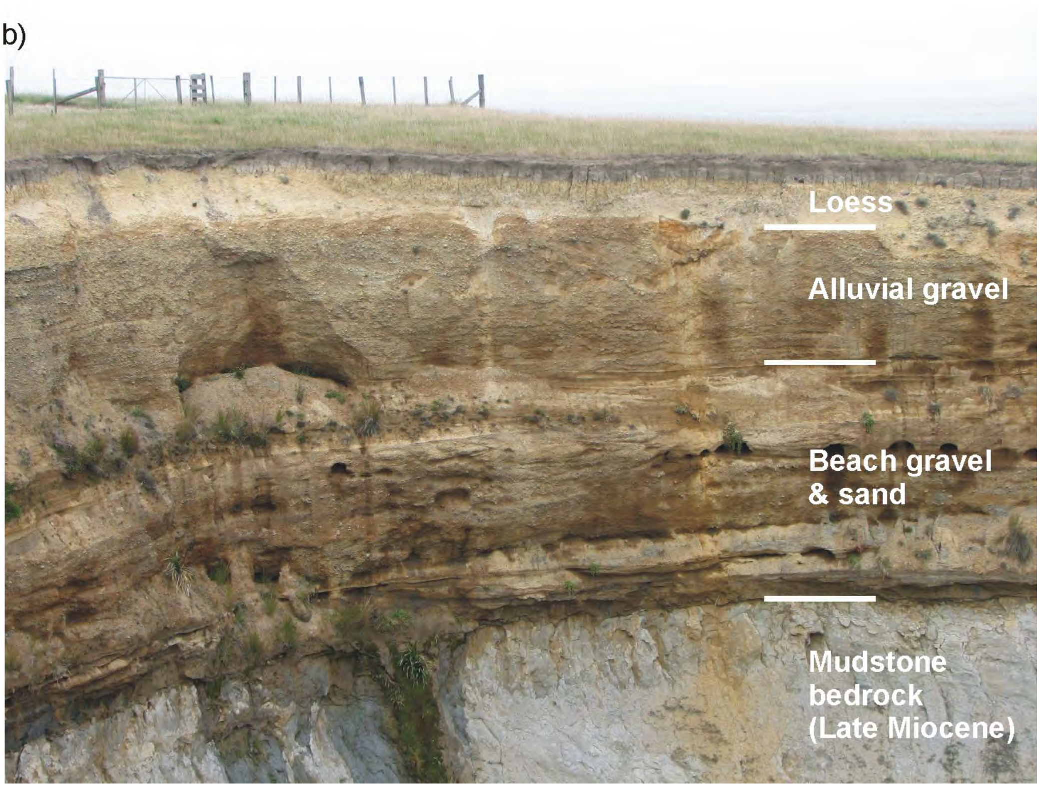


**Figure 27**. Photographs of the stop 3 "Grand Canyon" gully exposure into an uplifted marine terrace at Whangaimoana Beach, east of Lake Ferry (see Fig 26 for location). b) shows a closeup of the terrace deposits shown in a), consisting of 7-8 m of marine terrace deposits and 5-6 m of coverbeds.

Figure 28 shows a preliminary profile along the Palliser Bay sea cliff (see Fig. 26 for location), constructed from RTK GPS measurements. The profile shows the terrace surface and the strath and thus between the two are the terrace beach and coverbed deposits. The divergence between the strath and the surface at either end reflects the greater thicknesses of alluvial fan coverbeds near the range fronts. Overall the profile shows a general tilt down to the northwest, with some minor disturbances at ~3100 m and ~10000 m reflecting a known fault and a potentially new fold respectively. The strath are poorly exposed on the west side of the valley, but our tentative interpretation is that the profile is of the same terrace, probably 125 ka in age. The mechanism or source of the uplift and tilting will be discussed at stop 4.

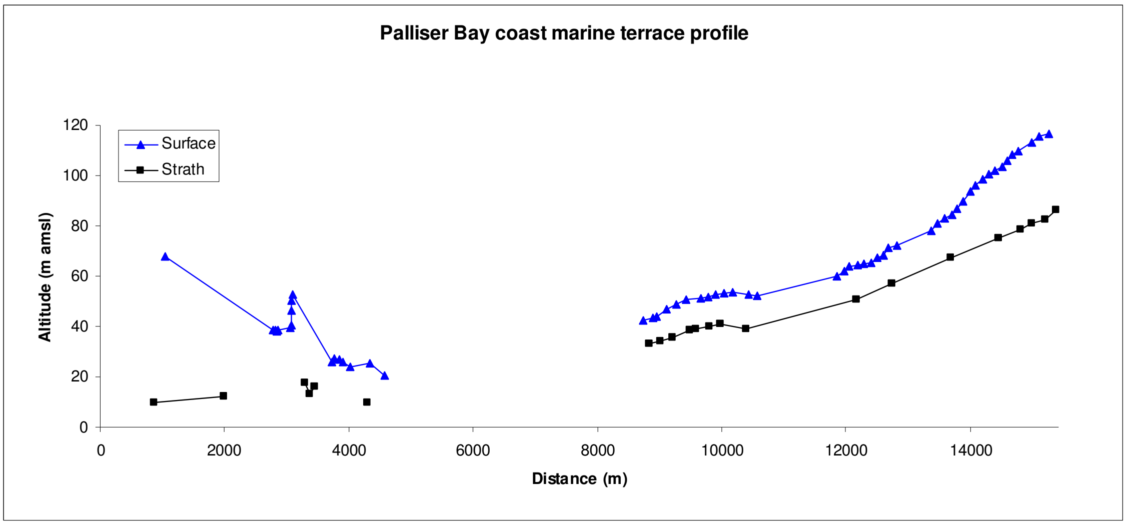


**Figure 28**. RTK GPS profile of the marine terrace surface and strath along the Palliser Bay coastal cliffs, located in Fig. 26.

**STOP 4. View of Pleistocene marine terraces, Te Kawakawa Rocks** *(near Ngawi and Cape Palliser).* **For location see Figures 12 and 13.**

*Drive to the parking area at Te Kawakawa Rocks, ~1.7 km past Ngawi, to see views of the marine terraces and the east coast of the North Island. Total time at this stop 30 mins.*

Along the drive from stop 3, the terraces steadily rise in altitude, with the last preserved terrace at Ngawi, at approximately 200 m amsl (Fig. 29, frontispiece a). Presumably terraces on the east coast have been eroded away. Tentative interpretations from recently acquired OSL ages suggest that the main terrace is likely to be the 125 ka terrace at stop 3.

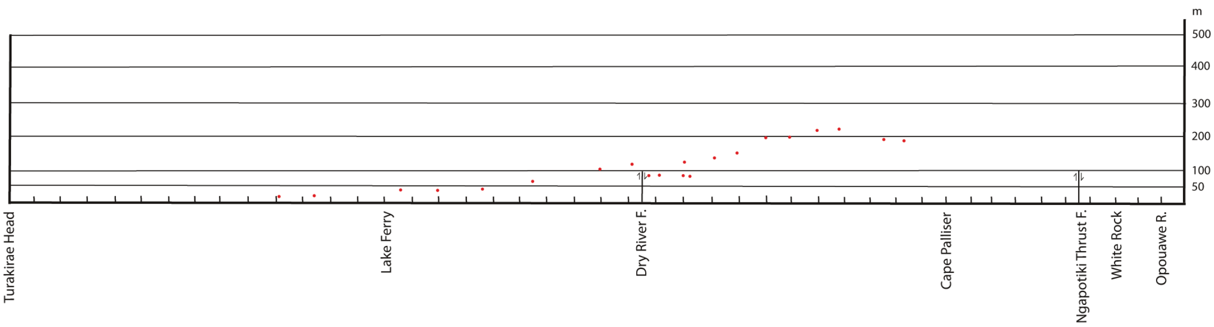


**Figure 29**. Marine terrace surface profile, compiled by Dee Ninis from published terrace mapping (Begg and Johnson, 2000) and topographic map data (1:50 000 scale maps). Terrace surfaces and straths have subsequently been surveyed with RTK GPS, but have not been plotted yet.

The relatively long (10's of km) wavelength over which the marine terraces are uplifted and tilted (Fig. 29) suggests that the uplift is unlikely to be related to individual (upper plate) faults. This has been tested with a dislocation model of uplift for the offshore, oblique, **Palliser-Kaiwhata Fault** (Fig. 30a). This model (see Fig. 30 caption for details) shows that as mapped, the fault is too far east to be the source of the marine terrace uplift, but even if it extends farther southwest, the uplift only extends <20 km inland. Incidentally, this model is consistent with fluvial terrace data from the lower Awhea River, shown by the green line (Litchfield and Wilson, in review).

The other candidate offshore fault is the **Boo Boo Fault** (Fig. 26), which is pure dextral strike-slip, so it also cannot be the source mechanism of the uplift.

Figure 30b also shows a dislocation model for rupture of the **Hikurangi subduction interface** (see Fig. 30 caption for details), based on the currently locked area determined from GPS studies (an updated version is shown in Fig. 31). Not surprisingly, this model shows uplift over a wider area, which appears to be more consistent with the pattern of uplift of the marine terraces. Is rupture of the subduction interface the uplift mechanism for the Palliser Bay coast marine terraces?

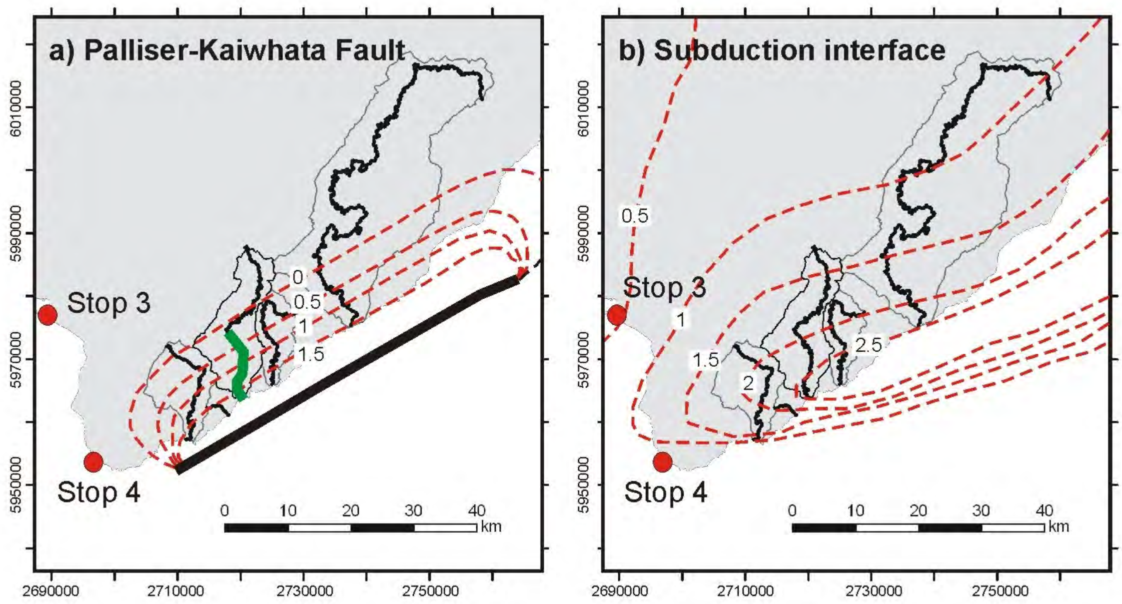


**Figure 30.** Dislocation models of possible uplift mechanisms for the marine terraces along the Palliser Bay coast. a) Model for oblique slip on the western part of the offshore Palliser-Kaiwhata Fault (Barnes and Audru, 1999), with a 40º dip, a down-dip depth of 10 km (to the subduction interface), and a net coseismic slip of 4 m, which was partitioned into 3.8 m dip-slip and 1.26 m strike-slip (i.e. a ratio of 4:3) (L. Wallace, pers. comm. 2008) b) Model for slip on the entire Hikurangi subduction interface (Power et al., 2008). The geometry and slip distribution is based on the GPS slip-defecit model of Wallace et al. (2004) (an updated version is shown in Fig. 31), and in this area the upper and lower depth are 6 and 40 km respectively, and the coseismic slip is ~6 m.

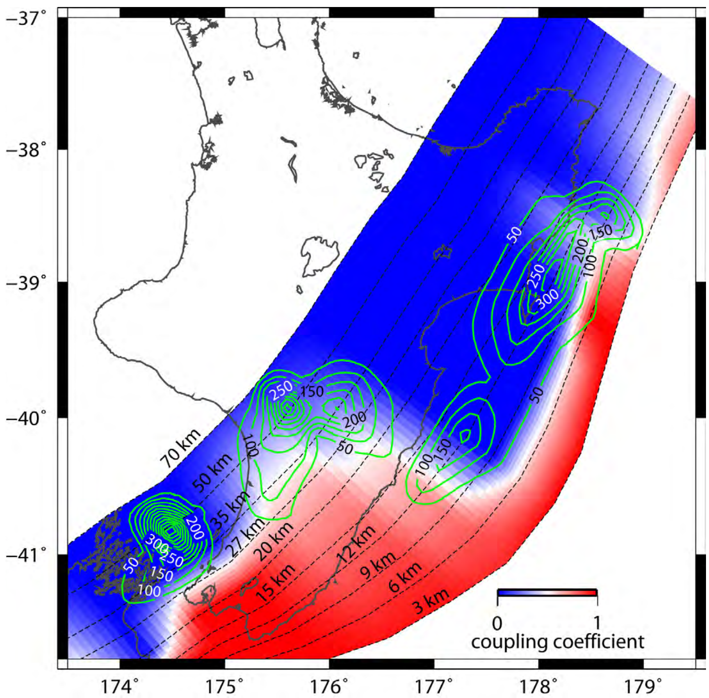


**Figure 31.** Interseismic coupling coefficient on the subduction interface determined from campaign GPS velocities in the North Island (e.g., Wallace et al., 2004) using the block modelling approach of McCaffrey (2002). Green contours show total slip (in mm) detected in episodic slow slip events on the Hikurangi subduction interface since 2002. Dashed black line shows depth contours (labelled) to the subduction interface (Wallace and Beavan, in prep.)

## References


Barnes, P.M., 2005, The southern end of the Wairarapa fault, and surrounding structures in Cook Strait, *in* Langridge, R., Townend, J., and Jones, A., eds., The 1855 Wairarapa Earthquake symposium--Proceedings Volume, Volume GW/RINV-T-05/205: Wellington, New Zealand, Greater Wellington Regional Council, p. 66-71.

Barnes, P. M., and Mercier de Lepinay, B., 1997, Rates and mechanics of rapid frontal accretion along the very obliquely convergent southern Hikurangi margin, New Zealand: Journal of Geophysical Research, v. 102, No. B11, p. 24,931-24,952.

Barnes, P.M., Mercier de Lépinay, B., Collot, J.-Y., Delteil, J., and Audru, J.-C., 1998, Strain partitioning in the transition area between oblique subduction and continental collision, Hikurangi margin, New Zealand: Tectonics, v. 17, p. 534-557

Barnes, P. M., and Audru, J.-C., 1999, Quaternary faulting in the offshore Flaxbourne and Wairarapa Basins, southern Cook Strait, New Zealand: New Zealand Journal of Geology and Geophysics, v. 42, p. 349-367.

Beanland, S., 1995, The North Island Dextral Fault Belt, Hikurangi Subduction Margin, New Zealand [Ph.D. thesis]: Wellington, New Zealand, Victoria University of Wellington.

Beanland, S., and Haines, J., 1998, A kinematic model of active deformation in the North Island, New Zealand, determined from geological strain rates: New Zealand Journal of Geology and Geophysics, v. 41, p. 311-324.

Beavan, J., Tregoning, P., Bevis, B., Kato, T., and Meertens, C., 2002, The motion and rigidity of the Pacific Plate and implications for plate boundary deformation: Journal of Geophysical Research, v. 107(B10), 2261, doi10.1029/2001JB000282.

Begg, J.G., and Mazengarb, C. 1996, Geology of the Wellington area, scale 1:50,000. Institute of Geological and Nuclear Sciences geological map 22.

Begg, J. G., and Johnston, M. R., 2000, Geology of the Wellington area, New Zealand: Institute of Geological and Nuclear Sciences, Ltd., Geological Map 64 (1:250,000).

Darby, D. J., and Beanland, S., 1992, Possible source models for the 1855 Wairarapa Earthquake, New Zealand: Journal of Geophysical Research, v. 97(B9), p. 12375-12389.

Darby, D.J., and Beavan, J. 2001, Evidence from GPS measurements for contemporary interplate coupling on the southern Hikurangi subduction thrust and for partitioning of strain in the upper plate: Journal of Geophysical Research, v.106, p. 30881-30891.

DeMets, C., Gordon, R.G., Argus, D.F. and Stein, S., 1990, Current plate motions. Geophysical Journal 101: 425-478.

DeMets, C., Gordon, R.G., Argus, D.F., Stein, S., 1994, Effect of recent revisions to the geomagnetic reversal time scale on estimates of current plate motions. Geophysical Research Letters 21: 2191-2194.

Downes, G., and Grapes, 1999, The 1855 Wairarapa Eathquake, New Zealand – historical data: GNS Science Report 99/16, 267 pp.

Dowrick, D.J., 1992, Attenuation of Modified Mercalli intensity in New Zealand earthquakes: Earthquake engineering and structural dynamics, v. 21, p. 182-196.

Formento-Trigilio, M.L., Burbank, D.W., Nicol, A., Shulmeister, J. & Rieser, U. 2002: River response to an active fold and thrust belt in a convergent margin setting, North Island, New Zealand. Geomorphology 49, 125-152.

Eade, R.E., 1995, Late Quaternary geology of the Wharekauhau area, Ocean Beach, Palliser Bay [BSc. (Hons) thesis]: Wellington, New Zealand, Victoria University of Wellington.

Ghani, M.A. 1978. Late Cenozoic crustal movements in the southern North Island, New Zealand. New Zealand Journal of Geology and Geophysics, v. 21, p. 117-125.

Grapes, R., 1999, Geomorphology of faulting: the Wairarapa fault, New Zealand: Z. Geomorphology, v. 115, p. 191-217.

Grapes, R., and Downes, G., 1997, The 1855 Wairarapa, New Zealand, earthquake-Analysis of historical data: Bulletin of the New Zealand National Society for Earthquake Engineering, v. 30, p. 271-368.

Grapes, R. H., and Wellman, H. W., 1988, The Wairarapa Fault: Victoria University of Wellington Geology Board of Studies, v. 4, p. 54.

Grapes, R., and Wellman, H. W., 1993, Wharekauhau Thrust (Palliser Bay) and Wairarapa Fault (Pigeon Bush) [Field-trip Guide]: Geological Society of New Zealand Miscellaneous Publication, v. 79B, p. 27-44.

Hull, A.G., and McSaveney, M., 1996, A 7000-year record of Great Earthquakes at Turakirae Head, Wellington, New Zealand, GNS Client Report 33493B, 10 p.
Kelsey, H.M., Cashman, S.M., Beanland, S., and Berryman, K.R., 1995, Structural evolution along the inner forearc of the obliquely convergent Hikurangi margin, New Zealand: Tectonics, v. 14, p. 1-18.
Kingma, J.T., 1967, Sheet 12, Wellington. Geological map of New Zealand, 1:250,000. Department of Scientific and Industrial Research, Wellington, New Zealand.
Lee, J. M., and Begg, J. G., 2002, Geology of the Wairarapa Area: Institute of Geological and Nuclear Sciences Limited: 1:250,000 Geological Map Series.
Little, T. A., Van Dissen, R., Schermer, E., Carne, R, 2009, Late Holocene surface ruptures on the southern Wairarapa fault, New Zealand: Link between earthquakes and the raising of beach ridges on a rocky coast: Lithosphere, v. 1., p. 1, paper no. L7R1.
Little, T. A., & Rodgers, D. W., 2005, Co-seismic slip during the 1855 earthquake, southern Wairarapa Fault, New Zealand: Proceedings Volume, The 1855 Wairarapa Earthquake Symposium, held at Museum of New Zealand Te Papa Tongarewa, September 8-10, 2005: Greater Wellington Regional Council, Publication No. GW/RINV-T-05/205, p. 11-20.
Hull, A.G. and McSaveney, M.J. 1996, A 7000-year record of great earthquakes at Turakirae Head, Wellington, New Zealand. GNS Client Report 33493B.10 (for Earthquake Commision).
Litchfield, N., Wilson, K. In review. Mechanisms of coseismic coastal uplift in the southern Hikurangi Margin: insights from Holocene terraces and dislocation modelling. Geomorphology.
Lyell, S.C., 1856, Sur les éffects du tremblement de terre du 23 Janvier, 1855 à la Nouvelle Zélande: Bull. Geol. Soc. France, Serie 2, 13, p. 661-667.
Lyell, C., 1868, "Principals of geology or the modern changes of the Earth and its inhabitants". 10th edition. London, England. John Murray.
Marra, M.J., 2003, Last interglacial beetle fauna from New Zealand: Quaternary Research, v. 59, p. 122-131.
McClymont, A.F., 2000, A gravity survey of the Wharekauhau Thrust, Palliser Bay, New Zealand. New Zealand Journal of Geology and Geophysics 43: 303-306.
McSaveney, M.J., Graham, I.J., Begg, J.G., Beu, A.G., Hull, A.G., Kim, Keong, Zondervan, A., 2006, Late Holocene uplift of beach ridges at Turakirae Head, south Wellington coast, New Zealand. New Zealand Journal of Geology and Geophysics. V. 49, p. 337-348.
Melhuish, A., Begg, J.G., Bannister, S., Mumme, T., 1997, Quaternary stratigraphy, structure, and deformation of the Upper Hutt Basin, Wellington, New Zealand. New Zealand Journal of Geology and Geophysics
Mouslopoulou, V., Nicol, A., Little, T.A., and Walsh, J., 2007, Displacement transfer between intersecting regional strike-slip and extensional fault systems: Journal of Structural Geology, v. 29, p. 100-116.
Nicol, A., Mazengarb, C., Chanier, F., Rait, G., Uruski, C., and Wallace, L., 2007, Tectonic evolution of the active Hikurangi subduction margin, New Zealand, since the Oligocene: Tectonics, v. 2, p. TC4002, doi: 10.1029/2006TC002090.
Nicol, A., Van Dissen, R., Vella, P., Alloway, B., and Melhuish, A., 2002, Growth of contractional structures during the last 10 m.y. at the southern end of the Hikurangi forearc basin, New Zealand: New Zealand Journal of Geology and Geophysics, v. 45, p. 365-385.
Ongley, M., 1943, Surface trace of the 1855 Earthquake: Trans. Roy. Soc. New Zealand, v. 73, p. 84-89.
Ota, Y., Williams, D. N., and Berryman, K., 1981, Late Quaternary tectonic map of New Zealand, Sheets Q27. R27 and R28, Wellington, scale 1:50,000, with notes: Lower Hutt, New Zealand Department of Scientific and Industrial Research
Power, W., Wallace, L., Reyners, M. 2008. Tsunami hazard posed by earthquakes on the Hikurangi subduction zone interface. GNS Science Consultancy Report 2008/40.
Reyners, M., 1998, Plate coupling and the hazard of large subduction thrust earthquakes at the Hikurangi subduction zone, New Zealand: New Zealand Journal of Geology and Geophysics, v. 41, p. 343-354.
Rollo, J., 1992, Geophysical investigations of the southwestern Wairarapa region of New Zealand. Unpublished MSc thesis, Victoria University of Wellington. Wellington, New Zealand.
Rowan, C. J., and Roberts, A. P., 2008, Widespread remagnetizations and a new view of Neogene tectonic rotations within the Australia-Pacific plate boundary zone, New Zealand: Journal of Geophysical Research, v. 113, p. doi: 10.1029/2006JB004594

Rodgers, D. W., and Little, T. A., 2006, World's largest coseismic strike-slip offset: The 1855 rupture of the Wairarapa Fault, New Zealand, and implications for displacement/length scaling of continental earthquakes: Journal of Geophysical Research, v. 111, p. B12408, doi:10.1029/2005JB004065.

Schermer, E. R., Van Dissen, R., Berryman, K. R., Kelsey, H. M., and Cashman, S. M., 2004, Active faults, paleoseismology, and historical fault rupture in northern Wairarapa, North Island: New Zealand Journal of Geology and Geophysics, v. 47, p. 107-122.

Schermer, L. Little, T. A., and Reiser, U., 2009, Long and short term deformation along the Wharekauhau thrust, North Island New Zealand: implications for an unstable linkage between active strike-slip and thrust faults: Tectonics, 28, TC6008, doi:10.1029/2008TC002426

Shulmeister, J. and Grapes, R.H., 2000, Gravel aggradation during interglaciations: implications from Palliser Bay, southern North Island, New Zealand. Geological Society of New Zealand. New Zealand Geophysical Society Joint Annual Conference, 27-30 November 2000. Geological Society of New Zealand Miscellaneous Publication 108A: p.140.

Shulmeister, J., Barrett, P., and Marra, M., 2000, Modern and ancient sedimentary environments of the southern Wairarapa: Geological Society of New Zealand Miscellaneous Publication, v. 108B, p. 1-15.

Sibson, R.H., 2006, Lyell and the 1855 Wairarapa earthquake in New Zealand: Recognition of fault rupture accompanying an earthquake: Seismological Research Letters, v. 77, p. 358-363.

Van Dissen, R. J., and Berryman, K. R., 1996, Surface rupture earthquakes over the last ~100 years in the Wellington region, New Zealand, and implications for ground shaking hazard: Journal of Geophysical Research, v. 101, p. 5999-6019.

Wallace, L.M. and R. J. Beavan, in prep. Diverse slow slip behavior on the Hikurangi subduction margin, New Zealand. JGR.

Wallace, L.M., Beavan, J., McCaffrey, R., and Darby, D., 2004, Subduction zone coupling and tectonic block rotations in the North Island, New Zealand: Journal of Geophysical Research, v. 109, p. 21.

Wang, N., 2001, Optically Stimulated Luminescence Dating Techniques and their Application to Dating the Loess in Southern North Island [M. Sc. thesis]: Victoria University of Wellington, 131 p.

Wang, N., and Grapes, R., 2007, Infrared-stimulated luminescence dating of late Quaternary aggradation surfaces and their deformation along an active fault, southern North Island of New Zealand: Geomorphology, v. doi:10.1016/j.geomorph.2007.07.016.

Warnes, P.N., 1989, The Quaternary geology of an area east of Carterton, Wairarapa Valley, New Zealand. Unpublished MSc thesis, Victoria University of Wellington. Wellington, New Zealand.

Wilson, C.J.N., Switsur, V.R., and Ward, A.P., 1988, A new 14C age for the Oruanui (Wairakei) eruption, New Zealand: Geological Magazine, v. 152, p. 297–300.